human hepatocytes obtained from one donor. Infection, extraction of serum samples, and sacrifice were performed under ether anesthesia. Mouse serum concentrations of human serum albumin (HSA) correlate with the repopulation index [11], and were measured as described previously [12]. The experimental protocol was approved by the Ethics Review Committee for Animal Experimentation of Graduate School of Biomedical Sciences, Hiroshima University.

2.2. HCV RNA transcription and inoculation into chimeric mice

A plasmid containing the full-length genotype 1a HCV cDNA clone, pCV-H77C, was kindly provided by Dr. Robert H. Purcell (National Institutes of Health). Ten micrograms of plasmid DNA, linearized by *Xba*I (Promega, Madison, WI) digestion, was transcribed in a 100-μl reaction volume with T7 RNA polymerase (Promega) at 37 °C for 2 h [13], and analyzed by agarose gel electrophoresis. Each transcription mixture was diluted with 400 μl of phosphate-buffered saline (PBS) and injected into the liver of chimeric mice. Transcripts of plasmid pJFH-1 containing the full-length HCV genotype 2a were transfected into Huh7 cells as described previously [6]. Seventy-two hours after transfection, 200 μl of the culture medium was injected intravenously into the chimeric mice. IFN-treatment was also performed by intramuscular injection of diluted IFN solutions. IFN-alpha was a kind gift from Hayashibara Biochemical Labs, Inc. (Okayama, Japan). Serum samples collected every 2 weeks after inoculation were frozen at −80 °C until further analysis.

2.3. Human serum samples

For control infection experiments, human serum containing a high titer of genotype 1b HCV (2.2×10^6 copies/ml) was obtained from a patient with chronic hepatitis after obtaining a written informed consent. The individual serum samples were divided into small aliquots and separately stored in liquid nitrogen until use.

2.4. RNA extraction and amplification

RNA was extracted from serum samples by Sepa Gene RV-R (Sankojunyaku, Tokyo), dissolved in 8.8 μl RNase-free H_2O, and reverse transcribed by using a random primer (Takara Bio, Inc., Shiga, Japan) and M-MLV reverse transcriptase (ReverTra Ace, TOYOBO Co., Osaka, Japan) in a 20 μl reaction mixture according to the instructions provided by the manufacturer. One microliter of cDNA solution was amplified by Light Cycler (Roche Diagnostic, Japan, Tokyo) for quantitation of HCV. The primers used for amplification were 5′-TTTATCCAAGAAAGGACCC-3′ and 5′-TTCACGCAGAAAGCGTCTAGC-3′. The amplification conditions included initial denaturation at 95 °C for 10 min, followed by 45 cycles of denaturation at 95 °C for 15 s, annealing at 55 °C for 5 s, and extension at 72 °C for 6 s. The lower detection limit of this assay is 10^3 copies/ml. Nested PCR was used with the outer primers NC1 (5′-CAACACTACTCGGCTAGCAGT-3′) and NC2 (5′-CCTGTGAGGAACTACTGTC-3′) and inner primers cc6 (5′-TTTATCCAAGAAAGGACCC-3′) and cc7 (5′-TTCACGCAGAAAGCGTCTAGCttc-3′). The amplification condition included 35 cycles of 94 °C for 30 s, 58 °C for 1 min 30 s, and 72 °C for 1 min after 5 min of initial denaturation at 94 °C followed by 7 min of final extension using Gene Taq (Wako Pure Chemicals, Tokyo) with anti-Taq high according to the instructions provided by the manufacturer (TOYOBO).

2.5. Histochemical analysis of mouse liver

Histopathological analysis and immunohistochemical staining using an antibody against HSA (Bethyl Laboratories Inc.) were performed as described previously [12].

3. Results

3.1. High serum HCV RNA titer in human hepatocyte chimeric mice after inoculation of serum samples obtained from HCV-infected patient

We inoculated 50 μl of genotype 1b serum samples into five chimeric mice intravenously to test their susceptibility to HCV infection. All mice became positive for HCV RNA by nested PCR at 2 weeks after inoculation (Fig. 1). The viremia reached a plateau level at 6–8 weeks after infection, and persisted for more than 12 weeks.

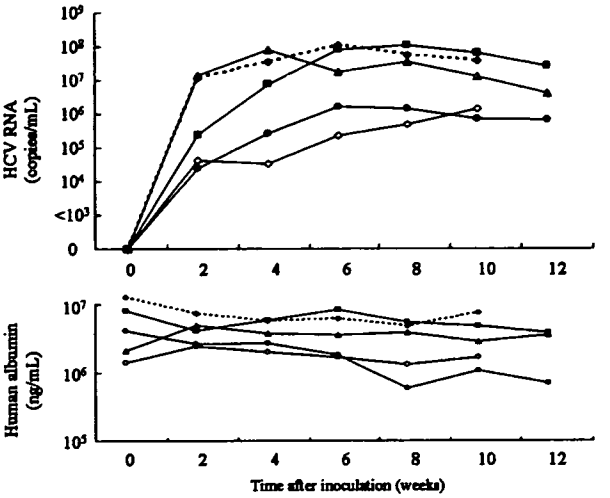

Fig. 1. Serial changes in HCV RNA and human serum albumin in sera of mice inoculated with human serum samples positive for genotype 1b HCV. Fifty microliter serum samples were injected intravenously into each mouse. Mice serum samples were obtained every 2 weeks after injection, and HCV RNA titer was analyzed.

3.2. Infection with in vitro-transcribed genotype 1a HCV RNA and cell culture generated genotype 2a HCV

In the next step, we tried to establish infection of cloned HCV using infectious genotype 1a and genotype 2a clones. In these experiments, we used two different strategies to establish infection using these two clones because genotype 1a has not been confirmed to replicate in cell culture system. We used genotype 1a HCV RNA (CV-H77C), which has been reported to be infectious to chimpanzee [13]. In vitro-transcribed HCV RNA was directly injected intrahepatically in three chimeric mice. We also infected three chimeric mice by intravenous injection of Huh7 cell-produced genotype 2a HCV after transfection of in vitro transcribed RNA from an infectious clone JFH-1. This clone has been shown to be infectious to a chimpanzee [6] and a chimeric mouse [7]. All mice developed measurable viremia 2 weeks after inoculation. At 6 weeks after inoculation, HCV RNA titer was 2.4×10^7 copies/ml (range: 8.8×10^6–2.9×10^7 copies/ml) in genotype 1a HCV-infected mice, and 2.5×10^5 copies/ml (range: 1.4×10^5–3.7×10^5 copies/ml) in genotype 2a HCV-infected mice (Fig. 2).

3.3. Passage experiment of HCV to naïve chimeric mice

We then performed passage experiments using naïve mice. Each of three mice was inoculated intravenously with 10 μl serum samples obtained from the above genotype 1a and genotype 2a HCV-infected mice at week 6. Two weeks after injection, all mice developed measurable viremia, and the titer was 8.5×10^6 copies/ml (range: 1.4×10^6–2.4×10^7 copies/ml) in genotype 1a, and 1.7×10^5 copies/ml (range: 1.5×10^5–2.5×10^5 copies/ml) in genotype 2a HCV-infected mice (Fig. 3).

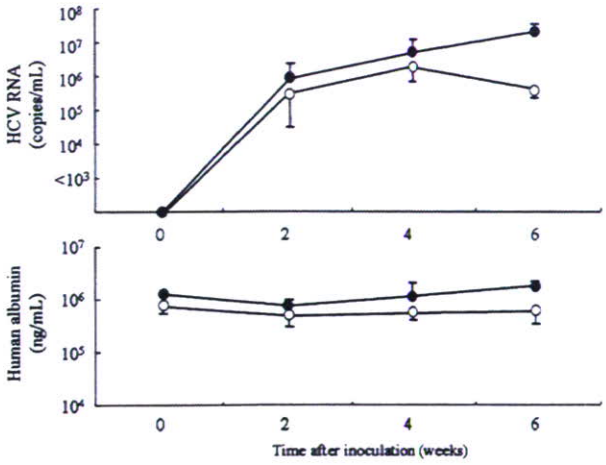

Fig. 2. Changes in HCV RNA and human albumin concentrations in serum of mice infected with clonal HCV. Each of three mice were inoculated intrahepatically with in vitro transcribed genotype 1a HCV RNA (closed circles) or intravenously with a culture medium collected from Huh7 cells transfected with JFH-1 genome intravenously (open circles). Data are mean ± S.D.

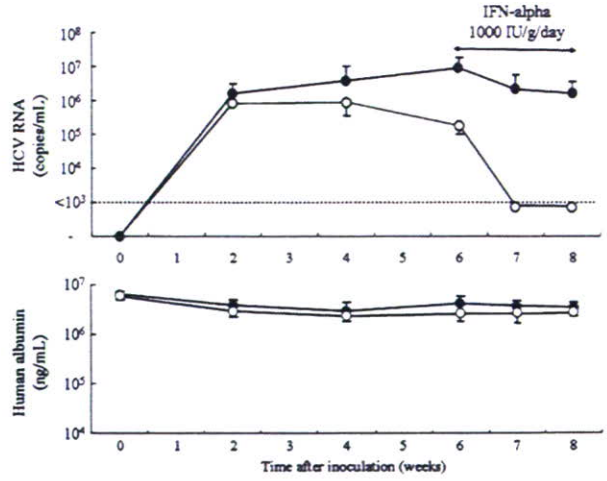

Fig. 3. Passage experiment and response to IFN-alpha therapy in mice infected with HCV genotypes 1a and 2a clones. Serum samples (10 μl) obtained from genotype 1a and 2a clonal HCV-infected mice sera (see Fig. 2) were inoculated intravenously into each of three naïve chimeric mice. Six weeks after infection, all six mice were injected intramuscularly with 1000 IU/g/day of IFN-alpha daily for 2 weeks. Closed circles: genotype 1a HCV-infected mice, open circles: genotype 2a HCV-infected mice. Data are mean ± S.D.

3.4. Variable susceptibility of HCV clones to IFN therapy

We treated each of the three mice infected with genotype 1a and 2a clones by passage experiments with 1000 IU/g of IFN-alpha daily for 2 weeks. Such treatment induced only a slight decrease in HCV in genotype 1a-infected mice; the viral load decreased only 0.6 and 0.7 log after 1 and 2 weeks of treatment, respectively (Fig. 3). In contrast, the same treatment reduced HCV genotype 2a RNA to undetectable levels after 1 and 2 weeks of IFN therapy. During IFN-treatment, serum HSA levels did not decrease in mice infected with genotype 1a or 2a HCV. Histopathological examination showed no morphological changes or apoptotic hepatocytes in replaced

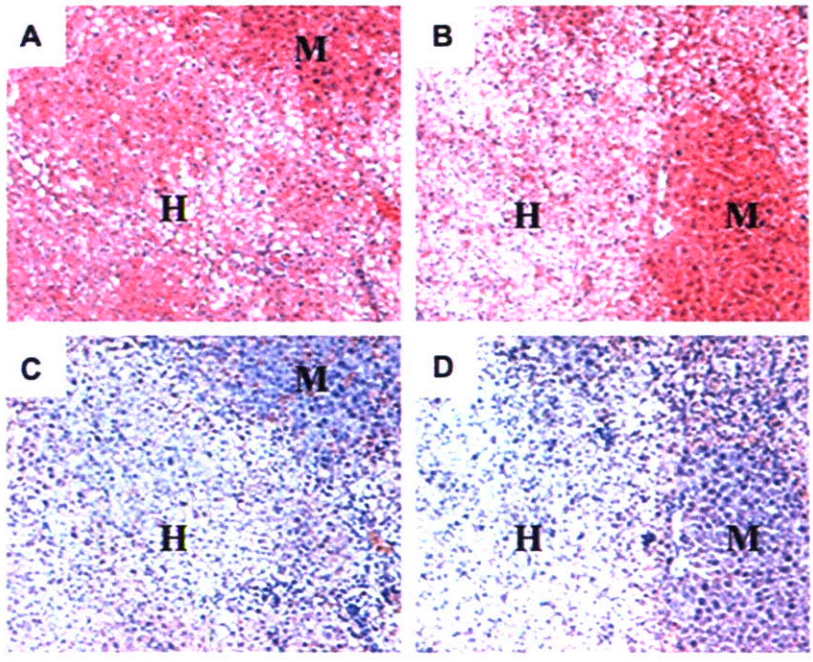

Fig. 4. Histochemical analysis of the tissues of infected chimeric mice. Liver samples obtained from mice infected with genotype 1a (A, C) and genotype 2a (B, D) stained with hematoxylin–eosin staining (A, B) or by immunohistochemical staining with anti-human serum albumin antibody (C, D). Regions are shown as human (H) and mouse (M) hepatocytes, respectively. (Original magnification, ×100.)

human hepatocytes in mice infected with each genotype after 2-week IFN-treatment (Fig. 4). These results suggest that the decrease in HCV is due to the direct anti-viral effect of IFN and not induced by liver cell damage. The difference in the virus titer and susceptibility to IFN are considered to be due to the characteristics of the genotypes.

4. Discussion

In this study, we established a reverse genetics system of HCV genotype 1a and 2a clones using human hepatocyte chimeric mice. The HCV genotype 2a clone, JFH-1, has remarkable features, i.e., infects cultured Huh7 cell line as well as establish infection in chimeric mouse [7]. It has been reported that HCV genotype 1a clone, H77-S, also infects Huh7 cell line and produces infectious virion [14]. In the present study, we intrahepatically inoculated genotype 1a infectious clone, CV-H77C. As reported in chimpanzee [13,15–17], we were able to establish genotype 1a infection using human hepatocyte chimeric mice. Using this technique, it is hoped that we can conduct further experiments in the future using genetically engineered HCV clones. Experiments using chimeric clone described by Lindenbach et al. [7] should also provide further information regarding the variable replication property of HCV genomes. Modifying genomes with nucleotide substitutions allowed examination of the functions of HCV peptides as we showed with HBV [12].

As reported recently by Kneteman et al. [10], the mouse model system is useful for evaluating the effect of anti-HCV drugs such as IFN, protease inhibitors and polymerase inhibitors. As we showed in this study, the response to IFN therapy varied according to HCV genotype. Further experiments are necessary to determine whether differences in response to IFN are due to the different replication ability (replication level of genotype 2a clone was slightly lower than that of genotype 1b, see Figs. 2 and 3) or differences in genotypes, as has been reported in clinical studies [18]. As we showed in this study (Fig. 4), there is no hepatocyte damage or inflammation in the liver of the infected chimeric mouse. Thus, this model is suitable for the study of mechanisms involved in HCV replication and IFN resistance.

The intrahepatic injection method used in this study simplified our experiments using genetically engineered virus. This is particularly important in studies of protease inhibitors and polymerase inhibitors because HCV will easily develop resistance against these small molecule agents.

Previous studies identified amino acid sequences that correlate with different susceptibilities of genotype 1b HCV against IFN therapy, namely, interferon sensitivity determining region [19] and the PKR-eIF2 phosphorylation homology domain [20,21]. To elucidate such issues, we are currently trying to establish genotype 1b infection system using the method described in this paper.

In summary, we showed in the present study the successful application of a genetically engineered HCV in human hepatocyte chimeric mice. Using this mouse model, we showed that genotypes 1a and 2a HCV clones exhibit different susceptibilities to IFN-alpha therapy. Our mouse model seems useful for the study of HCV virology and resistance of HCV against IFN and for the development of new anti-HCV therapy.

Acknowledgements: The authors thank Rie Akiyama, Kana Kunihiro and Kiyomi Toyota for their expert technical help, Dr. Robert H. Purcell and Dr. Jens Bukh for providing the full-length HCV cDNA clone of pCV-H77C. This study was supported in part by a Grant-in-Aid for Scientific Research from Japanese Ministry of labor, Health and Welfare.

References

[1] WHO. (1999) Global surveillance and control of hepatitis C. Report of a WHO Consultation organized in collaboration with the Viral Hepatitis Prevention Board, Antwerp, Belgium. J. Viral. Hepat. 6, 35–47.
[2] Kiyosawa, K., Sodeyama, T., Tanaka, E., Gibo, Y., Yoshizawa, K., Nakano, Y., Furuta, S., Akahane, Y., Nishioka, K. and Purcell, R.H. (1990) Interrelationship of blood transfusion, non-A, non-B hepatitis and hepatocellular carcinoma: analysis by detection of antibody to hepatitis C virus. Hepatology 12, 671–675.
[3] Niederau, C., Lange, S., Heintges, T., Erhardt, A., Buschkamp, M., Hurter, D., Nawrocki, M., Kruska, L., Hensel, F., Petry, W. and Haussinger, D. (1998) Prognosis of chronic hepatitis C: results of a large, prospective cohort study. Hepatology 28, 1687–1695.
[4] Fried, M.W., Shiffman, M.L., Reddy, K.R., Smith, C., Marinos, G., Goncales Jr., F.L., Haussinger, D., Diago, M., Carosi, G., Dhumeaux, D., Craxi, A., Lin, A., Hoffman, J. and Yu, J. (2002) Peginterferon alfa-2a plus ribavirin for chronic hepatitis C virus infection. N. Engl. J. Med. 347, 975–982.
[5] Zhong, J., Gastaminza, P., Cheng, G., Kapadia, S., Kato, T., Burton, D.R., Wieland, S.F., Uprichard, S.L., Wakita, T. and Chisari, F.V. (2005) Robust hepatitis C virus infection in vitro. Proc. Natl. Acad. Sci. USA 102, 9294–9299.
[6] Wakita, T., Pietschmann, T., Kato, T., Date, T., Miyamoto, M., Zhao, Z., Murthy, K., Habermann, A., Krausslich, H.G., Mizokami, M., Bartenschlager, R. and Liang, T.J. (2005) Production of infectious hepatitis C virus in tissue culture from a cloned viral genome. Nat. Med. 11, 791–796.
[7] Lindenbach, B.D., Meuleman, P., Ploss, A., Vanwolleghem, T., Syder, A.J., McKeating, J.A., Lanford, R.E., Feinstone, S.M., Major, M.E., Leroux-Roels, G. and Rice, C.M. (2006) Cell culture-grown hepatitis C virus is infectious in vivo and can be recultured in vitro. Proc. Natl. Acad. Sci. USA 103, 3805–3809.
[8] Shimizu, Y.K., Weiner, A.J., Rosenblatt, J., Wong, D.C., Shapiro, M., Popkin, T., Houghton, M., Alter, H.J. and Purcell, R.H. (1990) Early events in hepatitis C virus infection of chimpanzees. Proc. Natl. Acad. Sci. USA 87, 6441–6444.
[9] Mercer, D.F., Schiller, D.E., Elliott, J.F., Douglas, D.N., Hao, C., Rinfret, A., Addison, W.R., Fischer, K.P., Churchill, T.A., Lakey, J.R., Tyrrell, D.L. and Kneteman, N.M. (2001) Hepatitis C virus replication in mice with chimeric human livers. Nat. Med. 7, 927–933.
[10] Kneteman, N.M., Weiner, A.J., O'Connell, J., Collett, M., Gao, T., Aukerman, L., Kovelsky, R., Ni, Z.J., Zhu, Q., Hashash, A., Kline, J., His, B., Schiller, D., Douglas, D., Tyrrell, D.L. and Mercer, D.F. (2006) Anti-HCV therapies in chimeric scid-Alb/uPA mice parallel outcomes in human clinical application. Hepatology 43, 1346–1353.
[11] Tateno, C., Yoshizane, Y., Saito, N., Kataoka, M., Utoh, R., Yamasaki, C., Tachibana, A., Soeno, Y., Asahina, K., Hino, H., Asahara, T., Yokoi, T., Furukawa, T. and Yoshizato, K. (2004) Near completely humanized liver in mice shows human-type metabolic responses to drugs. Am. J. Pathol. 165, 901–912.
[12] Tsuge, M., Hiraga, N., Takaishi, H., Noguchi, C., Oga, H., Imamura, M., Takahashi, S., Iwao, E., Fujimoto, Y., Ochi, H., Chayama, K., Tateno, C. and Yoshizato, K. (2005) Infection of human hepatocyte chimeric mouse with genetically engineered hepatitis B virus. Hepatology 42, 1046–1054.
[13] Yanagi, M., Purcell, R.H., Emerson, S.U. and Bukh, J. (1997) Transcripts from a single full-length cDNA clone of hepatitis C virus are infectious when directly transfected into the liver of a chimpanzee. Proc. Natl. Acad. Sci. USA 94, 8738–8743.

[14] Yi, M., Villanueva, R.A., Thomas, D.L., Wakita, T. and Lemon, S.M. (2006) Production of infectious genotype 1a hepatitis C virus (Hutchinson strain) in cultured human hepatoma cells. Proc. Natl. Acad. Sci. USA 103, 2310–2315.
[15] Kolykhalov, A.A., Agapov, E.V., Blight, K.J., Mihalik, K., Feinstone, S.M. and Rice, C.M. (1997) Transmission of hepatitis C by intrahepatic inoculation with transcribed RNA. Science 277, 570–574.
[16] Yanagi, M., StClaire, M., Emerson, S.U., Purcell, R.H. and Bukh, J. (1999) In vivo analysis of the 3′ untranslated region of the hepatitis C virus after in vitro mutagenesis of an infectious cDNA clone. Proc. Natl. Acad. Sci. USA 96, 2291–2295.
[17] Beard, M.R., Abell, G., Honda, M., Carroll, A., Gartland, M., Clarke, B., Suzuki, K., Lanford, R., Sangar, D.V. and Lemon, S.M. (1999) An infectious molecular clone of a Japanese genotype 1b hepatitis C virus. Hepatology 30, 316–324.
[18] McHutchison, J.G., Gordon, S.C., Schiff, E.R., Shiffman, M.L., Lee, W.M., Rustgi, V.K., Goodman, Z.D., Ling, M.H., Cort, S. and Albrecht, J.K. (1998) Interferon alfa-2b alone or in combination with ribavirin as initial treatment for chronic hepatitis C. Hepatitis Interventional Therapy Group. N. Engl. J. Med. 339, 1485–1492.
[19] Enomoto, N., Sakuma, I., Asahina, Y., Kurosaki, M., Murakami, T., Yamamoto, C., Ogura, Y., Izumi, N., Marumo, F. and Sato, C. (1996) Mutations in the non-structural protein 5A gene and response to interferon in patients with chronic hepatitis C virus 1b infection. N. Engl. J. Med. 334, 77–81.
[20] Taylor, D.R., Shi, S.T., Romano, P.R., Barber, G.N. and Lai, M.M. (1999) Inhibition of the interferon-inducible protein kinase PKR by HCV E2 protein. Science 285, 107–110.
[21] Chayama, K., Suzuki, F., Tsubota, A., Kobayashi, M., Arase, Y., Saitoh, S., Suzuki, Y., Murashima, N., Ikeda, K., Takahashi, N., Kinoshita, M. and Kumada, H. (2000) Association of amino acid sequence in the PKR-eIF2 phosphorylation homology domain and response to interferon therapy. Hepatology 32, 1138–1144.

TOXICOLOGICAL SCIENCES 97(2), 533–538 (2007)
doi:10.1093/toxsci/kfm041
Advance Access publication March 6, 2007

Humanization of Excretory Pathway in Chimeric Mice with Humanized Liver

Hirotoshi Okumura,* Miki Katoh,* Toshiro Sawada,* Miki Nakajima,* Yoshinori Soeno,† Hikaru Yabuuchi,‡ Toshihiko Ikeda,§ Chise Tateno,¶ Katsutoshi Yoshizato,¶,‖ and Tsuyoshi Yokoi*,[1]

*Drug Metabolism and Toxicology, Division of Pharmaceutical Sciences, Graduate School of Medical Science, Kanazawa University, Kanazawa, Kakuma-machi, Kanazawa 920-1192, Japan; †PhoenixBio Co. Ltd, Hiroshima, Japan; ‡GenoMembrane Co. Ltd, Yokohama, Japan; §Drug Metabolism and Pharmacokinetics Research Laboratories, Sankyo Co. Ltd, Tokyo, Japan; ¶Hiroshima Prefectural Institute of Industrial Science and Technology, Cooperative Link of Unique Science and Technology for Economy Revitalization, Hiroshima, Japan; ‖Graduate School of Science, Hiroshima University, Hiroshima, Japan

Received February 3, 2007; accepted February 26, 2007

The liver of a chimeric urokinase-type plasminogen activator (uPA)$^{+/+}$/severe combined immunodeficient (SCID) mouse line recently established in Japan could be replaced by more than 80% with human hepatocytes. We previously reported that the chimeric mice with humanized liver could be useful as a human model in studies on drug metabolism and pharmacokinetics. In the present study, the humanization of an excretory pathway was investigated in the chimeric mice. Cefmetazole (CMZ) was used as a probe drug. The CMZ excretions in urine and feces were 81.0 and 5.9% of the dose, respectively, in chimeric mice and were 23.7 and 59.4% of the dose, respectively, in control uPA$^{-/-}$/SCID mice. Because CMZ is mainly excreted in urine in humans, the excretory profile of chimeric mice was demonstrated to be similar to that of humans. In the chimeric mice, the hepatic mRNA expression of human drug transporters could be quantified. On the other hand, the hepatic mRNA expression of mouse drug transporters in the chimeric mice was significantly lower than in the control uPA$^{-/-}$/SCID mice. In conclusion, chimeric mice exhibited a humanized profile of drug excretion, suggesting that this chimeric mouse line would be a useful animal model in excretory studies.

Key Words: biliary excretion; CMZ; renal excretion; transporter.

To clarify the pharmacokinetics of a drug is helpful to evaluate its therapeutic and toxicological effects. The pharmacokinetics is mainly determined by absorption, distribution, metabolism, and excretion. A drug is mostly eliminated by biliary and urinary excretion. To elucidate the excretory pathway of a drug is important for understanding the pharmacokinetics and toxicity. One of the major determinants of the excretory pathway of a drug is thought to be its molecular weight (Hirom *et al.*, 1972). In general, a drug with high molecular weight is mainly excreted via the bile duct. Recently, several adenosine 5′-triphosphate-binding cassette (ABC) transporters including P-glycoprotein (P-gp) and multidrug resistance–associated protein 2 (MRP2) have been shown to be relevant to biliary excretion (Chandra and Brouwer, 2004; Faber *et al.*, 2003). Various drug interactions in excretory pathways have been reported. Quinidine decreased the biliary clearance of digoxin by 42% in normal healthy human volunteers due to the inhibition of P-gp encoded by *multidrug resistance 1* (*MDR1*) gene (Angelin *et al.*, 1987). Probenecid decreased the clearance of irinotecan hydrochloride and increased the area under the curve of its metabolite by the inhibition of MRP2 in rats (Horikawa *et al.*, 2002). Thus, it is important to predict the drug interactions in excretion for avoiding adverse reactions.

In drug development, experimental animals have been used to predict the human excretory pathway of a drug candidate in preclinical studies. However, urinary recovery has been reported to be different between species in terms of ^{14}C-labeled compounds such as *N*-(2,6-dichlorobenzoyl)-4-(2,6-dimethoxyphenyl)-L-phenylalanine and zenarestat (Tanaka *et al.*, 1992; Tsuda-Tsukimoto *et al.*, 2005). The mechanism of such species differences is unclear, but may be partly due to differences in metabolism and excretion. For patient with liver or renal disease, it may be desirable to select a drug in consideration of its excretory pathway. Therefore, the elucidation of human excretory profile is necessary for preventing the condition to be worsened.

The livers of a chimeric urokinase-type plasminogen activator (uPA)$^{+/+}$/severe combined immunodeficient (SCID) mouse line established by Tateno *et al.* (2004) could be replaced by more than 80% with human hepatocytes. We previously investigated the expression of human drug metabolizing enzymes in the liver of the chimeric mice (Katoh *et al.*, 2004, 2005a,b,c). The purpose of the present study is to clarify the excretory profile of a drug and the effect of the replacement with human hepatocytes on drug excretion in the chimeric mice. The clarification of humanized excretion as well as metabolism in the chimeric mice can support an evaluation of the toxicity,

[1] To whom correspondence should be addressed. Fax: +81-76-234-4407. E-mail: tyokoi@kenroku.kanazawa-u.ac.jp.

TABLE 1
Chimeric Mice Used in Excretion Study

Number	hAlb[a] (mg/ml)	RI[b] (%)
1	4.3	60
2	7.9	80
3	8.0	80
4	9.2	80
5	9.8	80

[a]The hAlb concentration in blood of chimeric mice.
[b]RI was calculated as described by Tateno *et al.* (2004).

especially in liver toxicity. Cefmetazole (CMZ), which is one of the cephalosporin antibiotics, was used as a probe in this excretory study because CMZ is excreted in an unchanged form in humans and rodents. The excretory pathways of CMZ in humans and rats were different. Urinary excretion was dominant in humans (Ko *et al.*, 1989; Welage *et al.*, 1990), whereas biliary excretion was dominant in rats (Murakawa *et al.*, 1980). However, CMZ excretion in mice has not been studied. In our preliminary study, biliary excretion was major in mice as well as rats. Therefore, in the present study, the chimeric mice were employed to investigate the humanized type of excretion.

MATERIALS AND METHODS

Materials. CMZ and cefazolin were purchased from Sigma-Aldrich (St Louis, MO). All primers shown in Tables 2 and 3 were commercially synthesized at Hokkaido System Science (Sapporo, Japan). Human P-gp, human MRP2, rat breast cancer resistance protein (Bcrp), and rat bile salt export pump (Bsep) membranes were obtained from GenoMembrane (Yokohama, Japan) and ABC Transporter ATPase Assay Reagents Kit was purchased from Nacalai Tesque (Kyoto, Japan). All other chemicals were of the analytical or highest grade commercially available.

Animals. Animal maintenance and treatment were conducted in accordance with the National Institute of Health Guide for Animal Welfare in Japan, and the present study was approved by the Ethics Committees of Kanazawa University and the Hiroshima Prefectural Institute of Industrial Science and Technology Ethics Board. ICR mice (8 weeks old) were purchased from SLC Japan (Hamamatsu, Japan). Cryopreserved human hepatocytes from a donor (9-month-old, white, male) were purchased from In Vitro Technologies (Catonsville, MD). The chimeric mice were generated by the method described previously (Tateno *et al.*, 2004). Briefly, uPA$^{+/+}$/SCID mice at 20–30 days after birth were injected with human hepatocytes through a small left flank incision into the inferior splenic pole. When necessary, the chimeric mice were treated ip with nafamostat mesilate as described by Tateno *et al.* (2004). The treatment with nafamostat mesilate was discontinued more than 12 h before the excretion study. The concentration of human albumin (hAlb) in the blood of the chimeric mice and the replacement index (RI; the rate of replacement from mice to humans) were measured using an enzyme-linked immunosorbent assay and immunohistochemistry with anti-human specific cytokeratin 8 and 18 antibodies, respectively (Tateno *et al.*, 2004). There was a good correlation between the hAlb concentration and RI (Tateno *et al.*, 2004). The chimeric mice used in the present study were 12- to 17-week-old and exhibited more than 5 mg/ml hAlb concentrations or 60% of RI. The control uPA$^{-/-}$/SCID mice were obtained as previously reported (Tateno *et al.*, 2004).

TABLE 2
Sequence of Primers for Human Drug Transporters Used in the Present Study

Primer	Sequence
MDR1 S	5′-GGTACCATACAGAAACTCTT-3′
MDR1 AS	5′-TACAACTTCACCAAATGTG-3′
BSEP S	5′-TGAGCCTGGTCATCTTGTG-3′
BSEP AS	5′-TCCGTAAATATTGGCTTTCTG-3′
MRP2 S	5′-ACTATGGGCTGATATCCAG-3′
MRP2 AS	5′-CAGAATTCATCACAAACGCA-3′
BCRP S	5′-GCAGACTTCTTCTTGGACA-3′
BCRP AS	5′-TGATGACAGAAGGAGGTGGT-3′
OCT1 S	5′-GTACCTGTGGTTCACGGACT-3′
OCT1 AS	5′-CCAGGCAGATCATTTGTATTG-3′
OATP1B1 S	5′-GGGATCTCTGTTTTCTAAAATG-3′
OATP1B1 AS	5′-TCCAGCACATGCAAAGACAG-3′
OATP1B3 S	5′-GTCCAGTCATTGGCTTTGCA-3′
OATP1B3 AS	5′-TTATTTGGATTTTTCGGCAAG-3′

Note. S, sense primer; AS, antisense primer.

CMZ excretion in ICR mice. To clarify CMZ excretion in mice and evaluate the pathway of administration, ICR mice were ip ($n = 6$) and iv ($n = 6$) administered with CMZ in phosphate-buffered saline (PBS) (pH 7.4) at a dose of 25 mg/kg. Urine and feces samples were collected during 24 h after the CMZ administration. The samples were frozen at − 20°C until analysis.

CMZ excretion in chimeric mice. Chimeric mice ($n = 5$, Table 1) and control uPA$^{-/-}$/SCID mice ($n = 7$) were ip administered with CMZ in PBS (pH 7.4) at a dose of 25 mg/kg. Urine and feces samples were collected during 24 h after the CMZ administration. The samples were frozen at − 20°C until analysis.

Quantification of CMZ. The CMZ in urine and feces was quantified using high-performance liquid chromatography (HPLC) (Welage *et al.*, 1990). Urine samples (0.1 ml) were diluted with 0.4 ml of distilled water. Feces samples were homogenized by Polytoron homogenizer (OMNI international, Marietta, GA) with distilled water and centrifuged at 1,500 × g for 10 min. The diluted

TABLE 3
Sequence of Primers for Mouse Drug Transporters Used in the Present Study

Primer	Sequence
mdr1 S	5′-TACGACCCCATGGCTGGATC-3′
mdr1 AS	5′-GGTAGCGAGTCGATGAACTGG-3′
bsep S	5′-AAAATAATCCTGGAGTACTA-3′
bsep AS	5′-AGCCTTCTCCAGAATTTC-3′
mrp2 S	5′-GAGGCTACAGTCGATAACGA-3′
mrp2 AS	5′-ATAGTTCAATACGTAGAAGAT-3′
bcrp S	5′-GCGGATTTTTTCCTTGATGT-3′
bcrp AS	5′-AAAGAGGTAACATAGACTGG-3′
oct1 S	5′-GTATCTATGGTTCTCTTGTG-3′
oct1 AS	5′-AAGACAAGCGAGGGTCACA-3′
oatp1b2 S	5′-ATATGTAGACCTGAGAAGTG-3′
oatp1b2 AS	5′-ATGCTTCTCAGAGACCATAG-3′

Note. S, sense primer; AS, antisense primer.

TABLE 4
Hepatic mRNA Expression of Human Transporters in Chimeric Mice with Humanized Liver

Human transporter	Relative mRNA expression
MDR1	2.39 ± 0.90
BSEP	0.41 ± 0.11
MRP2	0.73 ± 0.17
BCRP	5.84 ± 3.49
OCT1	2.19 ± 0.59
OATP1B1	1.58 ± 0.36
OATP1B3	0.58 ± 0.13

Note. Data represent the mean ± SD of seven mice. Relative mRNA expression was calculated as described in "Materials and Methods" section.

TABLE 5
Hepatic mRNA Expression of Mouse Transporter in Chimeric Mice with Humanized Liver

Mouse transporter	Relative mRNA expression
mdr1	2.03 ± 0.61
bsep	0.27 ± 0.18
mrp2	0.16 ± 0.10
bcrp	0.10 ± 0.07
oct1	0.04 ± 0.03
oatp1b2	0.05 ± 0.04

Note. Data represent the mean ± SD of seven mice. Relative mRNA expression was calculated as described in Materials and Methods section.

urine (0.5 ml) and the supernatant of the feces (0.5 ml) samples were treated with 0.5 ml of 0.5% trichloroacetic acid in methanol containing cefazolin (20 nmol) as an internal standard. After incubation at − 20°C for 20 min, the mixture was centrifuged at 15,000 × g for 10 min. Then the supernatant was diluted 1:1 with 0.1 M citrate buffer (pH 5.4). Aliquots of 50 µl of the sample were injected to the HPLC system with a C_{30} 5-µm analytical column (Develosil, 4.6 × 150 mm; Nomura Chemical, Aichi, Japan). The mobile phase was acetonitrile:0.01 M citrate buffer (pH 5.4) = 8:92 (vol/vol), and the flow rate was 1.2 ml/min. The column temperature was 35°C. The eluate was monitored at 254 nm.

Hepatic RNA extraction and real-time RT-PCR. Human and mouse transporter mRNAs in chimeric mice were quantified by real-time RT-PCR. Total hepatic RNA was extracted using ISOGEN (Nippon Gene, Tokyo, Japan), and cDNAs were synthesized as described previously (Iwanari *et al.*, 2002). The sequences of primers for human or mouse transporters are shown in Tables 2 and 3, respectively. PCR was performed using the Smart Cycler (Cepheid, Sunnyvale, CA). After initial denaturing at 95°C for 30 s, amplification was started by denaturation at 94°C for 4 s, and then annealing and extension was performed simultaneously. The conditions of the one-step annealing and extension were as follows: human MDR1, human BCRP, human organic anion transporting polypeptide (OATP) 1B1, mouse mdr1, mouse mrp2, mouse organic cation transporter 1 (oct1), and mouse oatp1b2: 64°C for 20 s for 45 cycles; human MRP2: 64°C for 20 s for 35 cycles; human BSEP, human OCT1, human OATP1B3, and mouse bcrp: 66°C for 20 s for 45 cycles; mouse bsep: 60°C for 20 s for 45 cycles.

Amplified products were monitored directly by measuring the increase in the dye intensity of SYBR Green I (Molecular Probes, Eugene, OR) that binds to double-strand DNA amplified by PCR. The copy number of mRNA in the cDNA sample was calculated using the standard amplification curve. It was confirmed that the primers for human and mouse transporters used in this study did not cross-react with mouse mRNA and human mRNA, respectively. The primer set of mouse mdr1 reacts with both mdr1a and mdr1b. For the investigation of mRNA expression of human and mouse transporters, the numbers of the chimeric mice and control uPA$^{-/-}$/SCID mice used were seven and five, respectively (Tables 4 and 5). For human transporter, the mRNA expression level in chimeric mice was calculated as the relative mRNA expression to the donor hepatocytes (Table 4). For mouse transporter, the mRNA expression level in chimeric mice was calculated as relative mRNA expression to control uPA$^{-/-}$/SCID mice (Table 5).

Drug-stimulated transporter ATPase activity assay. The drug-stimulated transporter ATPase activity was measured using ABC Transporter ATP Assay Reagents Kits as described by Ohashi *et al.* (2006) with slight modifications. Briefly, human P-gp, human MRP2, rat Bsep, and rat Bcrp membranes (20 µg) were preincubated at 37°C for 5 min in 40 µl of reaction buffer and CMZ in the presence or absence of 500 µM sodium orthovanadate in 96-well plates. The reaction was initiated by the addition of 20 µl of 12mM MgATP solution and was terminated 30 min later by the addition of 30 µl of stop solution (10 wt/vol% lithium lauryl sulfate). Two hundred microliters of detection reagent (8% ascorbic acid, 0.8% ammonium molybdate, and 3 mM zinc acetate) was added and incubated at 37°C for 20 min. The inorganic phosphate complex was detected by its absorbance at 665 nm and was quantitated by comparing the absorbance with a phosphate standard. The vanadate-sensitive ATP hydrolysis was determined by subtracting the value obtained with the vanadate-coincubated membrane fraction from vanadate-free membrane fraction.

RESULTS

Excretion of CMZ in ICR Mice

By iv administration of CMZ, the means of the 24-h cumulative urinary and fecal excretions were 32.4 ± 4.7 and 63.1 ± 6.6% of the dose, respectively. On the other hand, by ip administration of CMZ, the means of the 24-h cumulative urinary and fecal excretions were 36.9 ± 9.3 and 56.7 ± 8.5% of the dose, respectively. The biliary excretion of CMZ was clarified to be dominant in mice. The 24-h urinary and fecal excretions were similar between iv and ip administrations.

Excretion of CMZ in Chimeric Mice

The recovery of CMZ in urine and feces up to 24 h in chimeric mice is shown in Figure 1. In all of the chimeric mice, the excretion of CMZ in urine was significantly higher than that in feces. On the other hand, in control uPA$^{-/-}$/SCID mice, the excretion of CMZ in urine was significantly lower than that in feces. The means ± SD of the 24-h cumulative urinary and fecal excretions were 81.0 ± 9.5 and 5.9 ± 4.7% of the dose, respectively, in chimeric mice and 23.7 ± 8.8 and 59.4 ± 11.0% of the dose, respectively, in control uPA$^{-/-}$/SCID mice. The means of the total CMZ recovery were 86.9 ± 9.4 and 83.2 ± 13.3% of the dose in chimeric mice and the uPA$^{-/-}$/SCID mice, respectively.

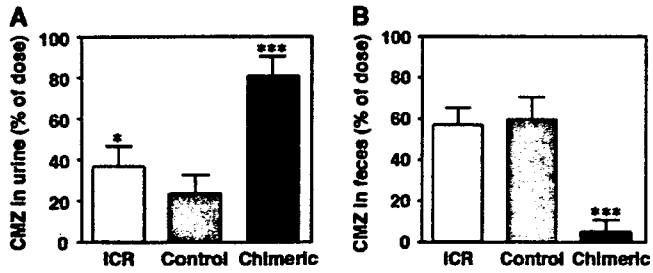

FIG. 1. CMZ excretion in chimeric mice with humanized liver. CMZ in urine (A) and in feces (B) was determined as described in "Materials and Methods" section. Data represent the mean ± SD. ICR, ICR mice ($n = 6$); control, uPA$^{-/-}$/SCID mice ($n = 7$); and chimeric, chimeric mice ($n = 5$). $*p < 0.05$, $***p < 0.001$, compared with control.

Expression of Human Drug Transporter in Chimeric Mice

The hepatic mRNA expression of human transporters in the chimeric mice is shown in Table 4. P-gp, BSEP, MRP2, and BCRP can transport a substrate into the bile duct from hepatocytes. OCT1, OATP1B1, and OATP1B3 can uptake a substrate into hepatocytes. Human transporters were expressed in the liver of all chimeric mice used in this study (Table 4). Because the anti-human transporter antibodies commercially available cross-react with mouse orthologous transporters, the protein expression level could not be measured.

Expression of Mouse Drug Transporter in Chimeric Mice

The hepatic mRNA expression of mouse transporters in the chimeric mice is shown in Table 5. The hepatic mRNA expression of mouse mdr1, bsep, mrp2, and bcrp in chimeric mice was 190, 31, 19, and 20% of that in control uPA$^{-/-}$/SCID mice, respectively. The mRNA expression of mouse oct1 and oatp1b2 in chimeric mice was 4 and 4% of that in uPA$^{-/-}$/SCID mice, respectively.

Drug-Stimulated Transporter ATPase Activity Assay

The affinity of CMZ to human P-gp and MRP2 was estimated by ATPase activity assay. No stimulation of vanadate-sensitive P-gp or MRP2 ATPase activity was observed up to 2 mM CMZ. Although human BCRP and BSEP membranes could not be obtained, CMZ did not stimulate the ATPase activity in rat Bcrp and Bsep membranes up to 1 mM CMZ.

DISCUSSION

Understanding the pharmacokinetics could support the efficient and safe evaluation of drug candidates during drug development. However, extrapolation from experimental animals to humans is difficult due to the species differences in absorption, distribution, metabolism, and excretion. There have been many reports that the cumulative excretion of radioactivity in urine and feces was different between species after administration of a ^{14}C-labeled drug (Karim *et al.*, 1976; Kolis *et al.*, 1976). In the present study, we focused on the species differences in excretion. In the case of CMZ, an unchanged form is mainly excreted. In humans, the cumulated CMZ excretion in urine was 79.7 ± 13.4% of the dose for 72 h after iv administration (Welage *et al.*, 1990) and was 68.8–86.0% of the dose for 24 h after im administration (Ko *et al.*, 1989). On the other hand, CMZ was mainly excreted into bile in rats (Murakawa *et al.*, 1980). In the preliminary study, the major excretory pathway was biliary excretion in ICR mice. Taking this information into consideration, CMZ was selected to investigate the humanization of the excretion pathway in chimeric mice. In humans, CMZ is usually administered iv. In mice, the CMZ excretion showed no significant difference between iv and ip administration. Therefore, excretion after an ip administration of CMZ was measured in the present study. In control uPA$^{-/-}$/SCID mice, biliary excretion of CMZ was the major pathway, reflecting the species differences in CMZ excretion between humans and mice. In chimeric mice, CMZ was mainly excreted in urine (Fig. 1). The present results suggested that the excretory profile of CMZ was humanized in the chimeric mice. The replacement with human hepatocytes of mouse liver seemed to affect the excretory profile of the drugs.

Recently, many drug transporters have been clarified to play important roles in drug excretion. In the present study, the expression of human and mouse drug transporters was investigated in the chimeric mice. In biliary excretion, the roles of human MDR1, BSEP, MRP2, and BCRP have been well characterized and were shown to be expressed on the canalicular membrane of hepatocytes. Human OCT1, OATP1B1, and OATP1B3 on the sinusoidal membrane, which may be involved in the uptake of a drug into hepatocytes, were also investigated. Human drug transporters were expressed in the liver of the chimeric mice, which was consistent with the previous report by Nishimura *et al.* (2005). For some human transporters, the relative mRNA expression in the chimeric mice was higher or lower than that in the donor hepatocytes. The mechanism of this phenomenon was unclear. Further study is needed to clarify the expression of human transporters in the chimeric mice generated using hepatocytes from various donors. In addition, the expressions of mouse drug transporters in chimeric mice were measured. Mouse oatp1b2 may correspond to human OATP1B1 (Hagenbuch and Meier, 2004). The expressions of mouse bsep, mrp2, bcrp, oct1, and oatp1b2 mRNAs in chimeric mice were lower than those in control uPA$^{-/-}$/SCID mice. The mRNA expression of some mouse cytochrome P450 enzymes in chimeric mice was described by Nishimura *et al.* (2005). The expression ratios of Cyp1a2, Cyp2c9, Cyp2e1, and Cyp3a11 mRNA, of which the mouse mRNA in chimeric mice to that in uPA$^{-/-}$/SCID mice, were 0.19 or less (Nishimura *et al.*, 2005). Their result was similar to those in our analysis. In the present study, the relative expressions in four out of six mRNAs were 0.20 or less (Table 5). It is presumed that 20% or less of mouse mRNA may be expressed in chimeric mice compared with

control uPA$^{-/-}$/SCID mice. The livers of the chimeric mice used in the present study were replaced approximately 80% by human hepatocytes; therefore, the residue of mouse mRNA was thought to be reasonable. Further study is needed to clarify whether the mouse protein retains its activity. Both the reduction of mouse transporter and the increase of human transporter expressions would be related to the humanization of excretory pattern in the chimeric mice.

The mRNA expression of human BCRP in chimeric mice was higher than that in donor hepatocyte. The mRNA expression of mouse mdr1 in chimeric mice was higher than that in control uPA$^{-/-}$/SCID mice. These results may be caused by the procedure of the generation of the chimeric mice or the knocking of the uPA gene, but the mechanism is unclear. It was clarified that CMZ was not a human P-gp and rat Bcrp substrate by the measurement of the ATPase activity using human P-gp and rat Bcrp. Therefore, the changes of the CMZ excretory profile in chimeric mice may be independent of the mouse mdr1 and human BCRP mRNA. The drug transporter for CMZ has not been identified yet. However, it should be possible that humanized drug transporters may influence the excretion in the chimeric mice. Although the present study did not investigate the humanization of other factors such as the physiology of liver and bile flow, we keep it in mind to discuss the mechanism.

There are a few reports on the species differences of the expression and substrate specificity in drug transporters. BCRP mRNA could be expressed in both liver and kidney in mice (Jonker *et al.*, 2000; Shimano *et al.*, 2003), but in liver and not in kidney in humans (Doyle *et al.*, 1998). Some compounds exhibited differences in the transport ratio between human and mouse P-gps (Yamazaki *et al.*, 2001). Taking the species differences of drug transporters into consideration, the chimeric mice could make some contribution to the understanding of drug transport involved in the excretion.

In conclusion, the excretory pattern of CMZ could be humanized in chimeric mice, suggesting that the chimeric mice can be useful in studies on drug excretion as well as drug metabolism. Further study concerning drug transporters is needed, but the present study would provide valuable information for applying pharmacological studies using chimeric mice with humanized liver.

ACKNOWLEDGMENTS

This work was supported by a Research on Advanced Medical Technology, Health, and Labor Sciences Research Grant from the ministry of Health, Labor, and Welfare of Japan. We acknowledge Mr Brent Bell for reviewing the manuscript.

REFERENCES

Angelin, B., Arvidsson, A., Dahlqvist, R., Hedman, A., and Schenck-Gustafsson, K. (1987). Quinidine reduces biliary clearance of digoxin in man. *Eur. J. Clin. Invest.* **17,** 262–265.

Chandra, P., and Brouwer, K. L. (2004). The complexities of hepatic drug transport: Current knowledge and emerging concepts. *Pharm. Res.* **21,** 719–735.

Doyle, L. A., Yang, W., Abruzzo, L. V., Krogmann, T., Gao, Y., Rishi, A. K., and Ross, D. D. (1998). A multidrug resistance transporter from human MCF-7 breast cancer cells. *Proc. Natl. Acad. Sci. U.S.A.* **95,** 15665–15670.

Faber, K. N., Muller, M., and Jansen, P. L. (2003). Drug transport proteins in the liver. *Adv. Drug Deliv. Rev.* **55,** 107–124.

Hagenbuc, B., and Meier, P. J. (2004). Organic anion transporting polypeptides of the OATP/SLC21 family: Phylogenetic classification as OATP/SLCO superfamily, new nomenclature and molecular/functional properties. *Pflugers Arch.* **447,** 653–665.

Hirom, P. C., Millburn, P., Smith, R. L., and Williams, R. T. (1972). Species variations in the threshold molecular-weight factor for the biliary excretion of organic anions. *Biochem. J.* **129,** 1071–1077.

Horikawa, M., Kato, Y., Tyson, C. A., and Sugiyama, Y. (2002). The potential for an interaction between MRP2 (ABCC2) and various therapeutic agents: Probenecid as a candidate inhibitor of the biliary excretion of irinotecan metabolites. *Drug Metab. Pharmacokinet.* **17,** 23–33.

Iwanari, M., Nakajima, M., Kizu, R., Hayakawa, K., and Yokoi, T. (2002). Induction of CYP1A1, CYP1A2, and CYP1B1 mRNAs by nitropolycyclic aromatic hydrocarbons in various human tissue-derived cells: Chemical-, cytochrome P450 isoform-, and cell-specific differences. *Arch. Toxicol.* **76,** 287–298.

Jonker, J. W., Smit, J. W., Brinkhuis, R. F., Maliepaard, M., Beijnen, J. H., Schellens, J. H., and Schinkel, AH. (2000). Role of breast cancer resistance protein in the bioavailability and fetal penetration of topotecan. *J. Natl. Cancer Inst.* **92,** 1651–1656.

Karim, A., Kook, C., Zitzewitz, D. J., Zagarella, J., Doherty, M., and Campion, J. (1976). Species differences in the metabolism and disposition of spironolactone. *Drug Metab. Dispos.* **4,** 547–555.

Katoh, M., Matsui, T., Nakajima, M., Tateno, C., Kataoka, M., Soeno, Y., Horie, T., Iwasaki, K., Yoshizato, K., and Yokoi, T. (2004). Expression of human cytochromes P450 in chimeric mice with humanized liver. *Drug Metab. Dispos.* **32,** 1402–1410.

Katoh, M., Matsui, T., Nakajima, M., Tateno, C., Soeno, Y., Horie, T., Iwasaki, K., Yoshizato, K., and Yokoi, T. (2005a). In vivo induction of human cytochrome P450 enzymes expressed in chimeric mice with humanized liver. *Drug Metab. Dispos.* **33,** 754–763.

Katoh, M., Matsui, T., Okumura, H., Nakajima, M., Nishimura, M., Naito, S., Tateno, C., Yoshizato, K., and Yokoi, T. (2005b). Expression of human phase II enzymes in chimeric mice with humanized liver. *Drug Metab. Dispos.* **33,** 1333–1340.

Katoh, M., Watanabe, M., Tabata, T., Sato, Y., Nakajima, M., Nishimura, M., Naito, S., Tateno, C., Iwasaki, K., Yoshizato, K., *et al.* (2005c). In vivo induction of human cytochrome P450 3A4 by rifabutin in chimeric mice with humanized liver. *Xenobiotica* **35,** 863–875.

Ko, H., Novak, E., Peters, G. R., Bothwell, W. M., Hosley, J. D., Closson, S. K., and Adams, W. J. (1989). Pharmacokinetics of single-dose cefmetazole following intramuscular administration of cefmetazole sodium to healthy male volunteers. *Antimicrob. Agents Chemother.* **33,** 508–512.

Kolis, S. J., Williams, T. H., and Schwartz, M. A. (1976). Identification of the urinary metabolites of ^{14}C-bumetanide in the rat and their excretion by rats and dogs. *Drug Metab. Dispos.* **4,** 169–176.

Murakawa, T., Sakamoto, H., Fukada, S., Nakamoto, S., Hirose, T., Itoh, N., and Nishida, M. (1980). Pharmacokinetics of ceftizoxime in animals after parenteral dosing. *Antimicrob. Agents Chemother.* **17,** 157–164.

Nishimura, M., Yoshitsugu, H., Yokoi, T., Tateno, C., Kataoka, M., Horie, T., Yoshizato, K., and Naito, S. (2005). Evaluation of mRNA expression of human drug-metabolizing enzymes and transporters in chimeric mouse with humanized liver. *Xenobiotica* **35,** 877–890.

Ohashi, R., Kamikozawa, Y., Sugiura, M., Fukuda, H., Yabuuchi, H., and Tamai, I. (2006). Effect of P-glycoprotein on intestinal absorption and brain penetration of antiallergic agent bepotastine besilate. *Drug Metab. Dispos.* **34,** 793–799.

Shimano, K., Satake, M., Okaya, A., Kitanaka, J., Kitanaka, N., Takemura, M., Sakagami, M., Terada, N., and Tsujimura, T. (2003). Hepatic oval cells have the side population phenotype defined by expression of ATP-binding cassette transporter ABCG2/BCRP1. *Am. J. Pathol.* **163,** 3–9.

Tanaka, Y., Sekiguchi, M., Sawamoto, T., Katami, Y., Ueda, T., Esumi, Y., and Noda, K. (1992). Absorption, distribution and excretion of zenarestat, a new aldose reductase inhibitor, in rats and dogs. *Xenobiotica* **22,** 57–64.

Tateno, C., Yoshizane, Y., Saito, N., Kataoka, M., Utoh, R., Yamasaki, C., Tachibana, A., Soeno, Y., Asahina, K., Hino, H., *et al.* (2004). Near completely humanized liver in mice shows human-type metabolic responses to drugs. *Am. J. Pathol.* **165,** 901–912.

Tsuda-Tsukimoto, M., Ogasawara, Y., and Kume, T. (2005). Pharmacokinetics and metabolism of TR-14035, a novel antagonist of a4ss1/a4ss7 integrin mediated cell adhesion, in rat and dog. *Xenobiotica* **35,** 373–389.

Welage, L. S., Borin, M. T., Wilton, J. H., Hejmanowski, L. G., Wels, P. B., and Schentag, J. J. (1990). Comparative evaluation of the pharmacokinetics of *N*-methylthiotetrazole following administration of cefoperazone, cefotetan, and cefmetazole. *Antimicrob. Agents Chemother.* **34,** 2369–2374.

Yamazaki, M., Neway, W. E., Ohe, T., Chen, I., Rowe, J. F., Hochman, J. H., Chiba, M., and Lin, J. H. (2001). In vitro substrate identification studies for P-glycoprotein-mediated transport: Species difference and predictability of in vivo results. *J. Pharmacol. Exp. Ther.* **296,** 723–735.

GH enhances proliferation of human hepatocytes grafted into immunodeficient mice with damaged liver

Norio Masumoto[1,2], Chise Tateno[1,3], Asato Tachibana[1,4], Rie Utoh[1], Yoshio Morikawa[4], Takashi Shimada[4], Hiroyuki Momisako[1,2], Toshiyuki Itamoto[2], Toshimasa Asahara[2,3] and Katsutoshi Yoshizato[1,3,5]

[1]Yoshizato Project, Cooperative Link of Unique Science and Technology for Economy Revitalization, Hiroshima Prefectural Institute of Industrial Science and Technology, 3-10-32 Kagamiyama, Higashihiroshima, Hiroshima 739-0046, Japan

[2]Division of Frontier Medical Science, Department of Surgery, Graduate School of Biomedical Sciences, Hiroshima University, 1-2-3 Kasumi, Minami-ku, Hiroshima 734-8551, Japan

[3]Hiroshima University Liver Project Research Center, 1-2-3 Kasumi, Minami-ku, Hiroshima 734-8551, Japan

[4]PhoenixBio Co. Ltd, 3-4-1 Kagamiyama, Higashihiroshima, Hiroshima 739-0046, Japan

[5]Developmental Biology Laboratory and Hiroshima University 21st Century COE Program for Advanced Radiation Casualty Medicine, Department of Biological Science, Graduate School of Science, Hiroshima University, 1-3-1 Kagamiyama, Higashihiroshima, Hiroshima 739-8526, Japan

(Correspondence should be addressed to K Yoshizato; Email: katsutoshi.yoshizato@phoenixbio.co.jp)

(C Tateno and K Yoshizato are now at PhoenixBio Co. Ltd, 3-4-1 Kagamiyama, Higashihiroshima, Hiroshima 739-0046, Japan)

(R Utoh is now at Institute of Advanced Life and Medical Sciences, Tokyo Women's Medical College, Kawada-chou 8-6, Shinjuku-ku, Tokyo 162-8666, Japan)

Abstract

We investigated effects of human (*h*) GH on the proliferation of *h*-hepatocytes that had been engrafted in the liver of albumin enhancer/promoter driven-urokinase plasminogen activator transgenic/severe combined immunodeficiency disease (uPA/SCID) mice (chimeric mice). The *h*-hepatocytes therein were considered to be deficient in GH, because *h*GH receptor (*h*GHR) is unresponsive to mouse GH. Actually, *h*IGF-1 was undetectable in chimeric mouse sera. The uPA/SCID mice were transplanted with *h*-hepatocytes from a 6-year (6Y)-old donor, and were injected with recombinant *h*GH (r*h*GH). r*h*GH stimulated the repopulation speed of *h*-hepatocytes; and up-regulated *h*IGF-1, human signal transducers and activators of transcription (*h*STAT) 3, and cell cycle regulatory genes such as human forkhead box M1, human cell division cycle 25A, and human cyclin D1. To confirm the reproducibility of these effects of r*h*GH, similar experiments were run using *h*-hepatocytes from a 46-year (46Y)-old donor. r*h*GH similarly enhanced their repopulation speed and up-regulated the expression of the above-tested genes, especially *h*IGF-1 and *h*STAT1. The extent of the enhancement by r*h*GH was much less than that in 6Y-hepatocyte-chimeric mice most probably due to the difference in GHR expression levels between the two donors. In conclusion, this study clearly demonstrated that r*h*GH stimulates the proliferation of *h*-hepatocytes *in vivo*.

Journal of Endocrinology (2007) **194**, 529–537

Introduction

Using rodents as experimental animals, it has been shown that differentiated hepatocytes can re-enter into the cell cycle when stimulated by growth factors, cytokines, and hormones (Taub 1996, Michalopoulos & DeFrances 1997, Fausto 2000). Hepatocytes in culture usually lose their replication ability and normal phenotypes and, thus, have had limited usability in testing the effects of these factors on hepatocytes. In addition, their effects on human (*h*)-hepatocytes *in vivo* have not been studied due to the lack of a suitable animal model. Previously, we developed a method to yield humanized mice (chimeric mice) whose liver is mostly replaced with *h*-hepatocytes (Tateno *et al.* 2004). The *h*-hepatocytes were transplanted into immunodeficient mice with diseased liver, albumin enhancer/promoter driven-urokinase plasminogen activator transgenic/severe combined immunodeficiency disease (uPA/SCID) mice. The transplanted cells were engrafted in the liver, continuously replicated, and repopulated in the liver. The extent of repopulation was calculated as the ratio (replacement index, RI) of the *h*-hepatocyte-repopulated area to the total examined area. Recent technological improvements enabled us to yield children's hepatocyte-chimeric mice with RI > 96%. The chimeric mice have been proven to be a useful animal model to examine biological and pathological features of *h*-hepatocytes *in vivo* (Tateno *et al.* 2004, Tsuge *et al.* 2005).

The regeneration capacity of rat liver decreases with age (Bucher *et al.* 1964, Stocker & Heine 1971), which is coincident with the fact that serum concentrations of growth

DOI: 10.1677/JOE-07-0126
0022-0795/07/0194-529 Online version via http://www.endocrinology-journals.org

hormone (GH) and insulin-like growth factor 1 (IGF-1) diminish with age (Kelijman 1991, Corpas *et al.* 1993), suggesting the association of GH with liver regeneration. Actually, evidence has been accumulating that GH is involved in liver regeneration and accounts for an aspect of age-dependent regenerative response of the liver in rodents (Krupczak-Hollis *et al.* 2003). However, the effects of GH on the growth of *h*-hepatocytes have not been studied *in vivo* at all yet. *h*GH is capable of stimulating rodent cells, whereas rodent GH cannot stimulate human cells because of its disability to bind to *h*GH receptors (*h*GHRs; Souza *et al.* 1995). Furthermore, it should be noted that *h*GH is not circulating in *h*-hepatocyte-chimeric mice, which indicates that *h*-hepatocytes in chimeric mice are in GH-deficient conditions. These facts and considerations strongly suggest that a chimeric mouse will provide an opportunity to examine the effects of *h*GH on growth of *h*-hepatocytes *in vivo*.

In this study, we examined the effects of *h*GH on the proliferation of *h*-hepatocytes using chimeric mice. The treatment of chimeric mice with *h*GH increased the repopulation speed and RI of transplanted *h*-hepatocytes, and up-regulated the GH-related signaling molecules. The present study shows that a *h*-hepatocyte-chimeric uPA/SCID mouse is a useful *in vivo* model to examine the effects of growth factors, cytokines, and hormones on *h*-hepatocytes.

Materials and Methods

Animals

The uPA/SCID mice weighing 6·3–10·0 g were produced as previously described (Tateno *et al.* 2004). The zygosity of the *uPA* transgene was determined by a multiplex PCR as previously described (Meuleman *et al.* 2003). Homozygous uPA/SCID mice were used as hosts throughout this study.

Transplantation of hepatocytes and bromodeoxyuridine (BrdU)-labeling

Cryopreserved *h*-hepatocytes from a 6-year-old Caucasian girl (6YG) and 46-year-old Caucasian man (46YM) respectively were purchased from *In vitro* Technologies (Baltimore, MD, USA) and thawed as previously described (Tateno *et al.* 2004). Trypan blue-exclusion test showed that the viability of 6YG- and 46YM-hepatocytes was 71·5±4·3% ($n=3$) and 72·2±2·3% ($n=3$) respectively. The *h*-hepatocytes (7·5 or $10·0\times10^5$ viable cells) were transplanted into the inferior splenic pole of uPA/SCID mice at 20–30 days after birth, through a small left-flank incision (Tateno *et al.* 2004). BrdU (Sigma Chemical Co.) was intraperitoneally injected into chimeric mice at a dose of 50 mg/kg body weight at 1 h before killing. Histological sections were prepared from the liver and stained with anti-BrdU antibodies as described below.

rhGH treatment

The 6YG- and 46YM-hepatocyte-chimeric mice were divided into two groups at 1 day post-transplantation; recombinant *h*GH (r*h*GH; Wako Pure Chemical Industries Ltd, Osaka, Japan)-treated (r*h*GH$^+$, experimental) and -untreated (r*h*GH$^-$, control) groups. r*h*GH was dissolved in water and used for animal injection. Animals of experimental groups were daily administered from day 1 after transplantation to 1 day before the day of killing with r*h*GH by subcutaneous injection at 2·5 μg/10 μl per g body weight.

Measurement of human albumin (hAlb) and human IGF-1 concentrations in mouse blood or sera

*h*Alb concentration in blood of a chimeric mouse is correlated with RI of transplanted hepatocytes (Tateno *et al.* 2004). Blood (2 μl) was collected from the tail vein of *h*-hepatocyte-chimeric mice. The blood *h*Alb concentrations were determined with a latex agglutination assay (Eiken Immunochemical Laboratory, Tokyo, Japan) or a *h*Alb ELISA quantitation kit (Bethyl Laboratories Inc., Montgomery, TX, USA). As a measure of GH/IGF-1 signaling in the chimeric mice, serum human IGF-1 (*h*IGF-1) concentrations were determined using a *h*IGF-I ELISA kit (R&D Systems Inc., Minneapolis, MN, USA).

Immunohistochemistry and measurement of RI

Frozen sections were prepared from chimeric livers, fixed in −20 °C acetone for 5 min and incubated with anti-human cytokeratin 8 and 18 (*h*CK8/18) antibodies (dilution, 1:25; MP Biomedicals, Aurora, OH, USA). The *h*CK8/18 antibodies reacted with *h*-hepatocytes but not with mouse (*m*)-hepatocytes. Formalin-fixed paraffin sections of chimeric livers were incubated with mouse anti-BrdU antibodies (dilution, 1:10; DakoCytomation, Glostrup, Denmark) and goat anti-*h*Alb antibodies (dilution, 1:1000; Bethyl Laboratories). The primary antibodies were visualized with a Vectastain ABC kit (Vector Laboratories, Burlingame, CA, USA) or peroxidase- and dextran-conjugated anti-mouse immunoglobulins (Dako Envision +; DakoCytomation) with 3, 3′-diaminobenzidine (Sigma) as substrates. The sections were counterstained with Mayer's hematoxylin. RI was calculated as the ratio of area occupied by *h*CK8/18-positive hepatocytes to the entire area examined on immunohistochemical sections of six lobes (Tateno *et al.* 2004). The ratios of BrdU-positive nuclei to *h*Alb-positive *h*-hepatocytes were determined by counting at least 1000 cells in 10 to 15 randomly selected vision fields in sections.

Quantification of mRNA in the livers of chimeric mice

Total RNAs were purified from liver tissues by an RNeasy mini kit (Qiagen). Using 1 μg total RNA by PowerScript reverse transcriptase (Clontech Inc.) and Random Primer oligonucleotides (Invitrogen Corp.), cDNAs were

synthesized according to the manufacturer's instruction. The mRNAs of genes shown in Table 1 were quantified in the liver tissues of chimeric mice by real-time RT-PCR (Tateno *et al.* 2004). Genes were amplified with a set of gene-specific primers shown in Table 1 and SYBR Green PCR mix (Applied Biosystems, Tokyo, Japan) in PRISM 7700 Sequence Detector (Applied Biosystems). We confirmed that these primers for *h*-genes amplified the *h*- but not the *m*-genes. Real-time RT-PCR was performed as follows: initial denaturation step at 95 °C for 10 min, followed by 40 cycles at 95 °C for 15 s and 60 or 62 °C for 1 min. All data were treated as previously described (Livak & Schmittgen 2001). The expression levels of the tested genes were normalized to the expression level of human glyceraldehyde 3-phosphate dehydrogenase (*hGAPDH*) gene and human hypoxanthine phosphoribosyltransferase 1 (*hHPRT-1*) gene.

Statistical analysis

Data were analyzed with StatView, 5.0 (SAS Institute Inc., Cary, NC, USA). Results are shown as the mean ± S.E.M. or S.D., and the significance of the difference between two groups under comparison was analyzed by Student's *t*-test when data were normally distributed and otherwise by Welch's test.

Results

Relationship of engraftment with repopulation of h-*hepatocytes*

In this study, we aimed to quantitatively assess the effect of r*h*GH on the extent of repopulation of *h*-hepatocytes in chimeric mice. It was considered that the number of engrafted *h*-hepatocytes depends on the number of the injected cells and affects the time length to reach the final (maximal) RI. Thus, we first examined the relationship between the number of the originally engrafted *h*-hepatocytes and that of the maximally repopulated *h*-hepatocytes, assuming that there is a linear relationship between the occupancy rate of *h*-hepatocytes after transplantation and the number of originally engrafted *h*-hepatocytes before the occupancy rate reaches the maximum when the repopulating *h*-hepatocytes terminate the proliferation (the saturation phase of the repopulation). Ten and 27 uPA/SCID mice were transplanted with 7·5 and $10{\cdot}0\times10^5$ 6YG-hepatocytes/animal respectively. All of the animals were successfully engrafted with *h*-hepatocytes. Blood *h*Alb levels were determined at 19–22 days post-transplantation as a measure of the number of the originally engrafted *h*-hepatocytes, and at 55–61 days as a measure of the number of the repopulated *h*-hepatocytes. The levels of '19–22 day'-group ($h\text{Alb}_{19\text{–}22}$) are plotted against those of '55–61 day'-group ($h\text{Alb}_{55\text{–}61}$; Fig. 1). The graph consisted of two regions, a near linear region in which $h\text{Alb}_{55\text{–}61}$ increased with $h\text{Alb}_{19\text{–}22}$ in a near linear fashion and a region of near plateau in which the increase of $h\text{Alb}_{19\text{–}22}$ did not meaningfully increase $h\text{Alb}_{55\text{–}61}$. It can be said that the plateau level (6–10 mg/ml) represented the maximal level (the maximal RI) of the occupancy of *h*-hepatocytes in the experimental conditions we adopted. In the case of $7{\cdot}5\times10^5$ cell transplantation, most chimeric mice showed $h\text{Alb}_{19\text{–}22}<0{\cdot}5$ mg/ml, and $h\text{Alb}_{55\text{–}61}$ was increased with the increase of $h\text{Alb}_{19\text{–}22}$. This result supported the above assumption that *h*-hepatocytes near lineally increased in number with the increase in the number of the originally engrafted *h*-hepatocytes and they did not reach the maximal repopulation state until 55–61 days post-transplantation. However, it should be noted here that the *h*Alb level does not correctly reflect the number of the repopulated *h*-hepatocytes as we showed in the previous study (Tateno *et al.* 2004) and also in the present study.

In contrast, in the case of $10{\cdot}0\times10^5$ cell transplantation, most of the chimeric mice showed $h\text{Alb}_{19\text{–}22}>0{\cdot}5$ mg/ml and reached the plateau level (>6 mg/ml) at 55–61 days, suggesting that there is an appropriate number of *h*-hepatocytes to be injected to obtain a high-engraftment rate (the number ratio of the engrafted *h*-hepatocytes to the injected *h*-hepatocytes). It is considered that the number of $7{\cdot}5\times10^5$ was smaller than this appropriate number. It appeared in $10{\cdot}0\times10^5$*h*-hepatocyte transplantation experiments that the proliferation of

Table 1 Oligonucleotide primers used in PCR amplification of growth hormone (GH)-related genes

Gene	Forward primer (5′–3′)	Reverse primer (5′–3′)
hGHR	TCACTCAAGGTTGAATCACAC	TCACATCAAGGTTGAATCACAC
hIGF-I	GCTTCCGGAGCTGTGATCTAA	GCTGACTTGGCAGGCTTG
hSTAT1	TTGCAGAACAGAGAACACGAGA	CATTCTGGGTAAGTTCAGTGAC
hSTAT3	GACCAACAATCCCAAGAATGTA	AATAATTCACACCAGGTCCCAA
hFoxM1	GCATCTACTGCCTCCCTGTG	GAGGAGTCTGCTGGGAACG
hCdc25A	CAAAGAGGAGGAAGAGCATGTC	CCAGGGATAAAGACTGATGAAGAG
hcyclin B1	CCTGATGGAACTAACTATGTTG	CATGTGCTTTGTAAGTCCTTGA
hcyclin D1	TGTGAAGTTCATTTCCAATCCG	CTGGAGAGGAAGCGTGTGAG
hCdk1	AAACTACAGGTCAAGTGG	GGGATAGAATCCAAGTATTTCTTCAG
hCdk2	ACAAGTTGACGGGAGAGGTG	CAGAAATTCAAAAACCAGGTAGAGT
hGAPDH	CCACCTTTGACGCTGGG	CATACCAGGAAATGAGCTTGACA
hHPRT1	TGGTCAGGCAGTATAATC	CAGTTTAGGAATGCAGCA

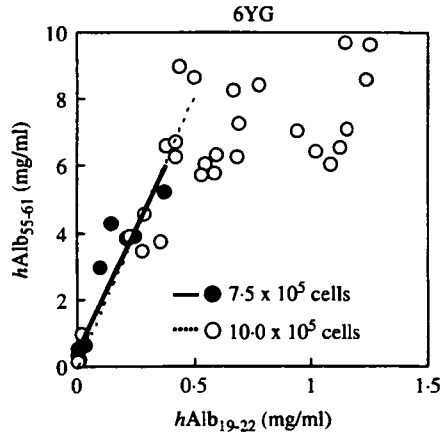

Figure 1 Relationship between *h*Alb concentrations in early and late time points after transplantation. uPA/SCID mice were transplanted with 7·5 (closed circles) and $10·0\times10^5$ 6YG-hepatocytes (open circles). *h*Alb levels at 19–22 days post-transplantation (hAlb$_{19–22}$) were plotted against those at 55–61 days (hAlb$_{55–61}$). The hAlb$_{55–61}$ in the $7·5\times10^5$ cell-transplantation experiment were lineally correlated with those at the hAlb$_{19–22}$ ($r^2=0·86$, solid line). The hAlb$_{55–61}$ in the $10·0\times10^5$ cell-transplantation experiment were also lineally correlated with hAlb$_{19–22}$ in the range <0·5 mg/ml of *h*Alb ($r^2=0·87$, dotted line).

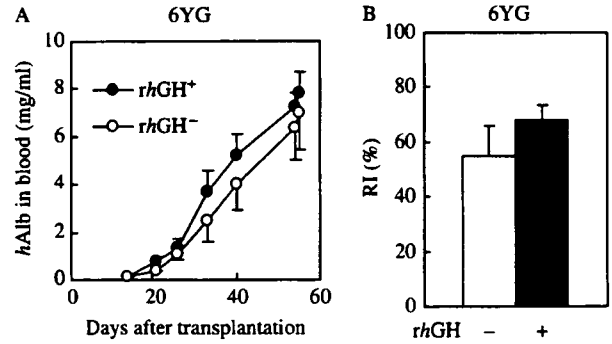

Figure 2 Repopulation of *h*-hepatocytes in uPA/SCID mice. Each uPA/SCID mouse was transplanted with $10·0\times10^5$ 6YG-hepatocytes. Animals in *rh*GH$^+$ group were daily injected with *rh*GH and *h*Alb concentrations in host blood were monitored (A). RIs of *rh*GH$^-$ (open bar)- and *rh*GH$^+$ 6YG-chimeric mice (closed bar) were determined at 55 days post-transplantation (B). Values represent the mean ± S.E.M. of three different mice.

h-hepatocytes terminated around 60 days post-transplantation when the *h*Alb level reached 6 mg/ml irrespective of hAlb$_{19–22}$, probably due to the contact inhibition among the *h*-hepatocytes, the toxicity of *h*-hepatocytes for the mouse when *h*Alb exceeded 6 mg/ml, and other yet unknown reasons. In $10·0\times10^5$ cell-transplantation experiments, there were several mice that showed hAlb$_{19–22}$<0·5 mg/ml. An apparent similar relationship between hAlb$_{19–22}$ and hAlb$_{55–61}$ was seen in these animals as in $7·5\times10^5$ *h*-hepatocyte transplantation experiments. Therefore, we empirically concluded that *h*-hepatocytes increased in number in an apparently quasilinear fashion after the engraftment from hAlb$_{19–22}$<0·5 mg/ml to hAlb$_{55–61}$<6 mg/ml. Thus, we utilized chimeric mice with hAlb$_{19–22}$<0·5 mg/ml for examining the effects of *h*GH on the proliferation of *h*-hepatocytes in the following experiments.

It has been generally recognized that *h*GH is capable of stimulating rodent cells, whereas rodent GHs are not able to bind to GHRs on *h*-hepatocytes (Souza *et al.* 1995). Six uPA/SCID mice were transplanted with $10·0\times10^5$ 6YG-hepatocytes/mouse. Half of them were treated with *rh*GH. The blood *h*Alb levels were monitored throughout the experimental period (up to 55 days) after transplantation (Fig. 2A). The concentrations of *h*Alb rapidly increased and exceeded 0·5 mg/ml (0·5–1·36 mg/ml) around 20 days post-transplantation in all mice irrespective of the treatment of *rh*GH and reached over 6 mg/ml around 50 days after transplantation. There were no differences in *h*Alb levels between *rh*GH$^-$ and *rh*GH$^+$ chimeric mice. At the end of this experiment, mice were killed for determining RI on immunohistological sections prepared from their liver tissues (Fig. 2B). Also, there were no differences in RIs between the two groups. Serum *h*IGF-1 levels were determined for mice from *rh*GH$^-$ and *rh*GH$^+$ groups. *h*IGF-1 was not detected in the animals of *rh*GH$^-$ groups whose *h*Alb concentrations were 8·2±1·1 mg/ml ($n=3$). In contrast *h*IGF-1 was detectable (11·9±11·2 mg/ml, $n=3$) in mice of *rh*GH$^+$ groups whose *h*Alb concentrations were 7·9± 1·9 mg/ml ($n=3$). Thus, the absence of *h*IGF-1 in sera of mice in *rh*GH$^-$ groups is explainable at least in part by assuming that *h*-hepatocytes did not respond to *m*GH in the chimeric mice, and when *rh*GH was given, *h*-hepatocytes responded to it and up-regulated *h*IGF-1 expression.

Enhancement of the repopulation of h*-hepatocytes by hGH*

Nine and eight uPA/SCID mice were transplanted with $7·5\times10^5$ 6YG- and $10·0\times10^5$ 46YM-hepatocytes/animal, then five and four of them were treated with *rh*GH respectively. Chimeric mice with both 6YG- and 46YM-hepatocytes showed variable *h*Alb levels, which were 0·01–0·6 and 0·0005–0·3 mg/ml at 20 days post-transplantation respectively. Three *rh*GH$^+$ and *rh*GH$^-$ mice with 0·01–0·05 mg/ml *h*Alb each were selected from 6YG- and 46YM-chimeric mice. The *rh*GH enhanced the increase of *h*Alb levels in both groups (Fig. 3). *rh*GH$^-$ animals slowly increased the values after 20 days post-transplantation, whereas *rh*GH$^+$ mice rapidly increased them in 6YG-chimeric mice (Fig. 3A). The transplanted cells in *rh*GH$^-$ 46YM-mice also slowly grew as in 6YG-mice (Fig. 3B). The *rh*GH also accelerated the repopulation in these mice, though its effect was considerably lower when compared with 6YG-hepatocyte mice.

The chimeric mice transplanted with 6YG- and 46YM-hepatocytes shown in Fig. 3A and B respectively were killed at 70 and 76 days post-transplantation for histological examinations respectively. There were no differences between *rh*GH$^+$ and *rh*GH$^-$ mice in body weight and liver size at the time of killing. *h*-Hepatocytes were immunohistochemically identified as *h*CK8/18-positive cells (Fig. 3C through F). Distributions of the immunopositive 6YG- and 46YM-cells in *rh*GH$^-$ animals are shown in Fig. 3C and E respectively. *h*-Hepatocyte colony

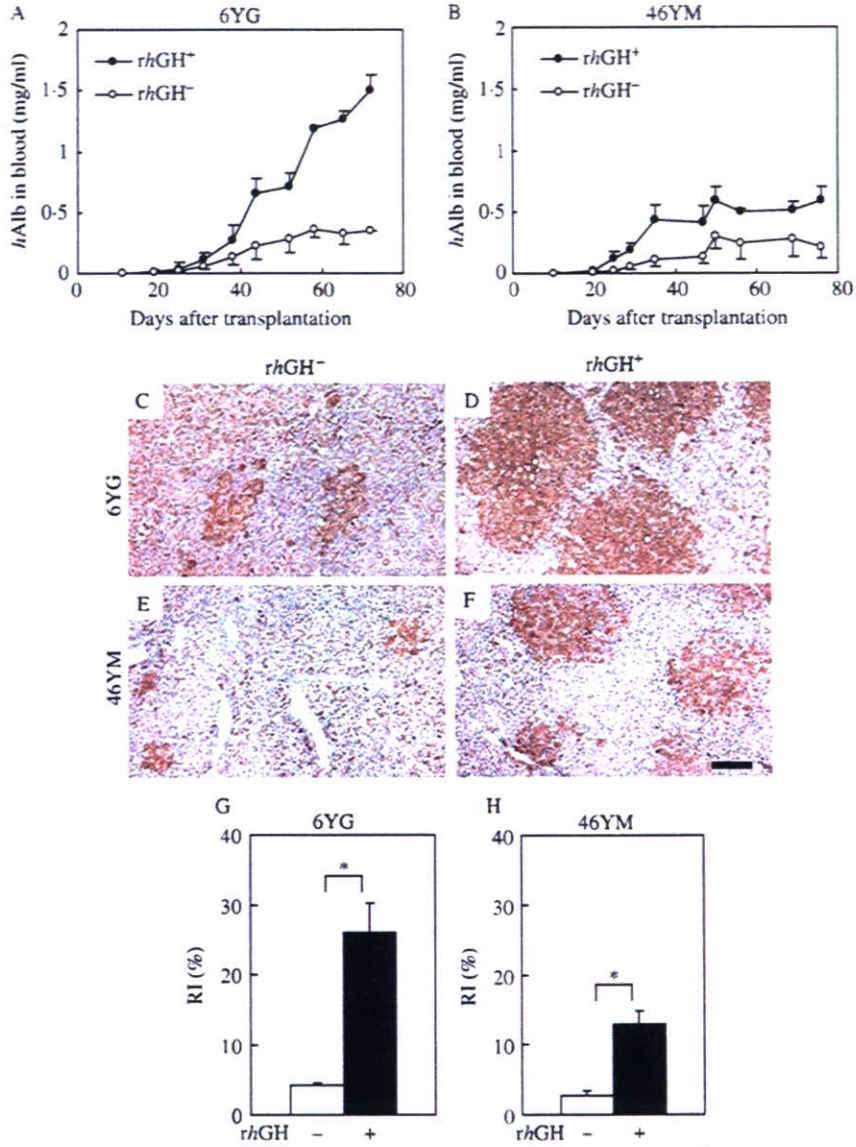

Figure 3 Effects of *h*GH on repopulation of *h*-hepatocytes. 6YG ($7{\cdot}5\times10^5$, A)- and 46YM ($10{\cdot}0\times10^5$, B)-hepatocytes were transplanted into each of uPA/SCIDmice and treated with *rh*GH as in Fig. 2. *h* Alb concentrations were monitored once a week. Solid and open circles show *rh*GH$^+$ and *rh*GH$^-$ mice respectively (C through F). Histological sections were prepared from six liver lobes of 6YG-chimeric mice at 70 days post-transplantation (C and D) and from those of 46YM-chimeric mice at 76 days post-transplantation (E and F). The sections were stained with anti-*h*CK8/18 antibodies. Sections 'C and E' and 'D and F' were from *rh*GH$^-$ and *rh*GH$^+$ mice respectively. The cytoplasm of hCK8/18-positive *h*-hepatocytes is stained brown. Scale bar in F: 20 μm (G and H). RI was calculated as the ratio of the brown colored areas to the examined total ones for 6YG- (G) and 46YM-chimeric mice (H). Open and closed bars show *rh*GH$^-$and *rh*GH$^+$ mice respectively. Values represent the mean ± S.E.M. of three different mice. Asterisks indicate significant differences (*$P<0{\cdot}05$, Student's *t*-test).

sizes were larger in 6YG- than in 46YM-hepatocytes. The size was greatly increased in *rh*GH$^+$ mice for both 6YG- (Fig. 3D) and 46YM-hepatocytes (Fig. 3F). *h*GH increased RI ~6·2- and 4·8-fold in 6YG-and 46YM-hepatocyte-chimeric mice respectively (Fig. 3G and H).

Effects of rhGH on DNA synthesis of h-hepatocytes in chimeric mice

We investigated whether *rh*GH stimulated the DNA synthesis of *h*-hepatocytes in chimeric mice. uPA/SCID mice were transplanted with 6YG- or 46YM-hepatocytes, injected with

*r*hGH, and were exposed with BrdU before killing at 2 weeks post-transplantation. BrdU-positive *h*-hepatocytes were often distributed in the peripheral regions of the colonies (Fig. 4A for 6YG-hepatocytes). The BrdU-labeling index of 6YG-hepatocytes in r*h*GH$^+$ mice was 2·2-fold higher ($P<0·05$) than that in r*h*GH$^-$ mice (Fig. 4B), indicating that GH induced the entry of *h*-hepatocytes into the S-phase of the cell cycle. The index of r*h*GH$^+$ 46YM-mice was 1·4-fold higher than that of r*h*GH$^-$ ones, but the difference was not significant.

Expression of hepatocyte growth-associated genes in chimeric livers

Previously, we showed the BrdU-labeling index of *h*-hepatocytes (9-month-old Caucasian boy) in chimeric mice at 1, 3, and 5 weeks post-transplantation was ~9, 5, and 2% respectively, and thereafter gradually decreased to <0·5% at 10–11 weeks (Emoto *et al.* 2005). Taking the present results shown in Fig. 4 and the above cited previous ones together, we considered that transplanted *h*-hepatocytes become most proliferative around 1 week post-transplantation, and, thus, hepatocyte growth-associated genes become activated then. However, there were not enough *h*-hepatocytes yet to yield sufficient RT-PCR amplification. Thus, we examined the effect of r*h*GH on the expression of hepatocyte growth-associated genes in *h*-hepatocytes of chimeric livers at 2 weeks point post-transplantation. Chimeric mice were treated with r*h*GH as in Fig. 4 and were killed at 2 weeks post-transplantation to determine mRNA levels of 10 genes by real-time RT-PCR: *h*GHR, *h*IGF-1, human signal transducers and activators of transcription (*h*STAT) 1, *h*STAT3, human forkhead box (*h*Fox) M1, human cell division cycle (*h*Cdc) 25A, *h*-cyclin B1, *h*-cyclin D1, human cyclin-dependent kinases (*h*Cdk) 1, and *hCdk2*. The expression levels were normalized to that of *hGAPDH* gene. The ratios of the expression under r*h*GH$^+$ to that under r*h*GH$^-$ are depicted as graphs for 6YG- (Fig. 5A) and 46YM-mice (Fig. 5B). r*h*GH did markedly increase *h*IGF-1 mRNA in both 6YG- (Fig. 5A) and 46YM-hepatocyte-chimeric mice (Fig. 5B; $P<0·05$, Student's *t*-test or Welch's test). The stimulation rate (9·1-fold) in 6YG-hepatocyte mice was much higher than that (2·6-fold) in 46YM-hepatocyte ones. The effects of r*h*GH were generally much prominent in chimeric mice bearing 6YG-hepatocytes as compared with that in those bearing 46YM-ones. In 6YG-hepatocyte-chimeric mice, r*h*GH significantly increased the expressions of mRNAs of *h*STAT3, *h*FoxM1, *h*Cdc25A, and *h*-cyclin D1 ($P<0·05$, Student's *t*-test, Fig. 5A). The expression levels for mRNAs of *h*STAT1, *h*-cyclin B1, *h*Cdk1, and *h*Cdk2 were higher in the r*h*GH$^+$- group than in r*h*GH$^-$ group in 6YG-hepatocyte-chimeric mice, although the difference in the ratio between the two groups was not significant. Similarly, mRNAs of *h*STAT1 and *h*STAT3 were induced by r*h*GH in 46YM-hepatocyte-chimeric mice, although the difference was not significant (Fig. 5B). In contrast to the expression in 6YG-chimeric mice, r*h*GH did not induce mRNAs of *h*FoxM1, *h*Cdc25A, *h*-cyclin B1, *h*-cyclin D1, *h*Cdk1, and *h*Cdk2 in 46YM-chimeric mice (Fig. 5B). 6YG-hepatocytes expressed *h*GHR mRNA at a 19·5-fold higher level than 46YM-hepatocytes in r*h*GH$^-$ group, suggesting differences in the responsiveness of these growth-related genes to r*hGH* might be due to the difference in GHR expression levels between the two donors. Similar results were obtained when the data were normalized by *h*HPRT-1 as another housekeeping gene.

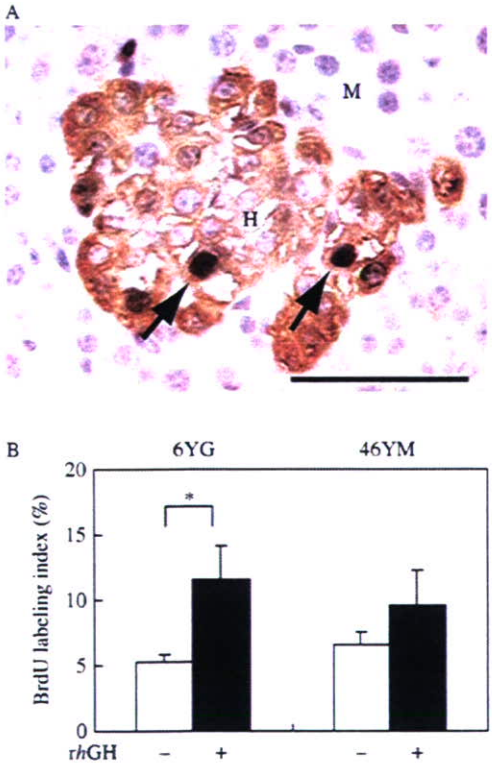

Figure 4 BrdU incorporation in the liver of chimeric mice. 6YG- and 46YM-hepatocytes were transplanted into uPA/SCIDmice, and they were treated with r*h*GH as in Fig. 2. They were injected with BrdU at 2 weeks post-transplantation, and killed 1 h later. A. The liver sections from a 6YG-chimeric mouse were subjected to double immunostaining with BrdU and *h*Alb. *h*Alb-positve *h*-hepatocytes have brown cytoplasm. BrdU-positive *h*-hepatocytes have dark brown nuclei (arrows). M and H indicate regions of *m*- and *h*-hepatocytes. Scale bar: 50 μm. B. BrdU-labeling index was calculated as the ratio of BrdU-positive nuclei to all the counted nuclei. Solid and open bars show r*h*GH$^+$ and r*h*GH$^-$ mice respectively. Values represent the mean±S.D. of experiments with 6YG- mice ($n=3$) and 46YM-mice ($n=4$). Asterisks indicate significant differences at * $P<0·05$ (Student's *t*-test).

Discussion

Hepatocytes of uPA/SCID mice undergo severe injury and, thus, genes of cytokines involved in liver regeneration are activated (Mars *et al.* 1995, Michalopoulos & DeFrances

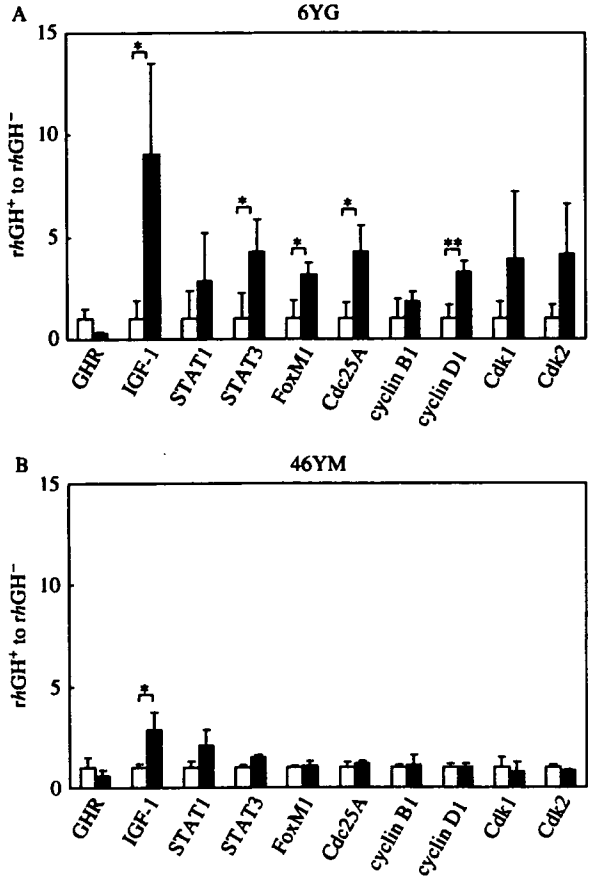

Figure 5 Expression of GH-related genes in chimeric mouse liver. Chimeric mice were yielded by transplanting 6YG- (A) and 46YM-hepatocytes (B), and treated with *rh*GH as in Fig. 2. The animals were killed at 2 weeks after transplantation. RNA was extracted from livers and used for determining the amount of mRNAs of ten genes, *h*GHR, *h*IGF-1, *h*STAT1, *h*STAT3, *h*FoxM1, *h*Cdc25A, *h*-cyclin B1, *h*-cyclin D1, *h*Cdk1, *h*Cdk2, and *h*GAPGH by real-time quantitative RT-PCR. Each data was divided by the data of *h*GAPDH. The graphs represent the ratio of the *rh*GH$^+$ to the *rh*GH$^-$ levels. Open and closed bars show *rh*GH$^-$ and *rh*GH$^+$ mice respectively. Values represent the mean±S.D. Asterisks indicate significant differences at $^*P<0{\cdot}05$ and $^{**}P<0{\cdot}01$.

1997). GH is one of such stimulators of liver regeneration in rodents (Krupczak-Hollis *et al.* 2003, Pennisi *et al.* 2004). Krupczak-Hollis *et al.* (2003) showed that GH promoted the proliferation of hepatocytes upon the partial hepatectomy in mice, which was mediated through activation of *FoxM1B* gene. Transgenic mice bearing GH-antagonist genes showed an incomplete liver regeneration and a reduced renewal rate of hepatocytes (Pennisi *et al.* 2004), suggesting a critical role of GH in liver regeneration. Regeneration-associated proliferation of hepatocytes in mice was impaired with a liver-specific IGF-1 receptor gene knockout (Desbois-Mouthon *et al.* 2006). In contrast to such abundant studies on rodents, there have been no studies on the effects of GH on *h*-hepatocytes *in vivo*. We undertook the present study assuming that a chimeric mouse will provide an opportunity to examine the effects of *rh*GH on proliferation of *h*-hepatocytes *in vivo*, because we considered that *h*-hepatocytes in chimeric mice are in GH-deficient conditions. This consideration was supported by the present study because we showed that *h*IGF-1 was actually undetectable in the chimeric mouse sera. We expected that *rh*GH treatment might enhance the proliferation of *h*-hepatocytes in uPA/SCID mice. Chimeric mice were yielded bearing *h*-hepatocytes from two donors whose sex and age were different, 6YG and 46YM, and were treated with *rh*GH. As a result, we were able to demonstrate for the first time that *rh*GH stimulates the proliferation of *h*-hepatocytes *in vivo*. This conclusion was reproducibly obtained from the two independent experiments using hepatocytes from different donors, although the extent of the stimulation was much higher for 6YG-hepatocytes than for 46YM-hepatocytes. This difference of GH-stimulation between the two donors might be explainable by the difference of GHR-expression level between them as shown in this study.

Studies on the molecular mechanisms of the action of GH are currently progressing in rodents. *c-fos* gene is an immediate early responsive gene to GH, which is mediated by STAT1 and STAT3 (Gronowski & Rotwein 1994, Gronowski *et al.* 1995, Herrington *et al.* 2000). Our study showed that *rh*GH increased the expression of *h*STAT1 and *h*STAT3 mRNAs in *h*-hepatocytes in chimeric mice. GH stimulates the growth of target cells through GHRs and its endocrine IGF-1 (Daughaday & Rotwein 1989). GH stimulates the synthesis and the secretion of IGF-1 by hepatocytes (Sjogren *et al.* 1999, Yakar *et al.* 1999). Secreted IGF-1 binds to the IGF-IR, which activates the expression of cell cycle-related genes such as cyclin D1 through ERK pathway (Desbois-Mouthon *et al.* 2006). Our present study showed that *rh*GH enhanced the expression of *h*IGF-I and cyclin D1 mRNAs in the liver of chimeric mice. Therefore, it is concluded that GH stimulates the growth of *h*-hepatocytes through activating GH/IGF-I/IGF-IR/ERK signaling. These results suggest that the stimulation of growth of hepatocytes by GH is induced through similar mechanisms in both rodents and humans. Studies remain to be done on the protein phosphorylation or the activation of the signaling cascades after the *rh*GH-stimulation using currently developed *h*-hepatocyte-chimeric mice.

It was shown in rodents that GH increases the FoxM1 level (Krupczak-Hollis *et al.* 2003), which stimulates the cell cycle progression at both the G1/S- and G2/M-phase transitions (Wang *et al.* 2001, 2002*a*,*b*, 2005, Major *et al.* 2004). Progression through the cell cycle is regulated by the temporal activation of multiple families of Cdk. Cdc25A, Cdc25B, and Cdc25C with phosphatase activities are involved in the activation of Cdks in a way that these enzymes dephosphorylate catalytic units of Cdks (Sebastian *et al.* 1993). Upon S-phase progression, Cdc25A phosphatase activates Cdk2-cyclin E by dephosphorylating inhibitory Cdk2 residues (Massague 2004). Progression through the

G2/M transition requires the activation of the Cdk1-cyclin B complex through dephosphorylation and the activation of Cdk1 by the Cdc25B and Cdc25C phosphatases, the latter of which is activated by Polo-like kinase 1 phosphorylation (Barr *et al.* 2004). It is noteworthy that r*h*GH up-regulated mRNAs of *h*FoxM1, *h*Cdc25A, *h*-cyclin B1, *h*-cyclin D1, *h*Cdk1, and *h*Cdk2 in 6YG-hepatocytes, but not 46YM-counterparts. Thus, it can be said that GH activates cell cycle progression of *h*-hepatocytes as known in rodents. The phosphorylation levels of Janus activating kinase 2 and GHR complex were decreased with age of rats (Xu *et al.* 1995). In the present study we showed that 6YG-hepatocytes expressed *h*GHR mRNA at much higher levels than 46YM-hepatocytes. This apparent age-dependent GH-expression level of *h*-hepatocytes should be tested in further studies with sufficient samples of donor hepatocytes for statistical treatments of the obtained results.

In this study we demonstrated usefulness of a *h*-hepatocyte-chimeric uPA/SCID mouse as an *in vivo* model to study effects of GH on the proliferation of *h*-hepatocytes. *h*-Hepatocyte-chimeric mice were also yielded using another type of immunodeficient and liver-injured mice obtained by crossing uPA-transgenic mice with mice whose recombinant activation gene-2 (RAG-2) had been deleted (Dandri *et al.*, 2001). It is worthy of examining in the future whether the effects of r*h*GH on *h*-hepatocytes observed in the present study can be reproduced in this uPA/RAG-2 mouse model. As clearly demonstrated for GH–GHR binding in the present study, *h*-hepatocytes in mice could be deficient for other growth factors and cytokines due to problems in interspecies ligand–receptor interaction. However, this limitation of *h*-hepatocyte-chimeric mice will provide us opportunities to study the mechanism of their interactions *in vivo* using chimeric mice in place of human body as exemplified for r*h*GH on *h*-hepatocytes in this study.

Acknowledgements

This study was supported by Cooperative Link of Unique Science and Technology for Economy Revitalization, Japan. We thank Y Yoshizane, H Kohno, Y Matsumoto, and S Nagai for breeding the mice and providing excellent technical assistance. The authors declare that there is no conflict of interest that would prejudice the impartiality of this scientific work.

References

Barr FA, Sillje HH & Nigg EA 2004 Polo-like kinases and the orchestration of cell division. *Nature Reviews. Molecular Cell Biology* **5** 429–440.

Bucher NL, Swaffield MN & DiTroia JF 1964 The influence of age upon the incorporation of thymidine-2-C14 into the DNA of regenerating rat liver. *Cancer Research* **24** 509–512.

Corpas E, Harman SM & Blackman MR 1993 Human growth hormone and human aging. *Endocrine Reviews* **14** 20–39.

Dandri M, Burda MR, Torok E, Pollok JM, Iwanska A, Sommer G, Rogiers X, Rogler CE, Gupta S, Will H *et al.* 2001 Repopulation of mouse liver with human hepatocytes and *in vivo* infection with hepatitis B virus. *Hepatology* **33** 1005–1006.

Daughaday WH & Rotwein P 1989 Insulin-like growth factors I and II. Peptide, messenger ribonucleic acid and gene structures, serum, and tissue concentrations. *Endocrine Reviews* **10** 68–91.

Desbois-Mouthon C, Wendum D, Cadoret A, Rey C, Leneuve P, Blaise A, Housset C, Tronche F, Le Bouc Y & Holzenberger M 2006 Hepatocyte proliferation during liver regeneration is impaired in mice with liver-specific IGF-1R knockout. *FASEB Journal* **20** 773–775.

Emoto K, Tateno C, Hino H, Amano H, Imaoka Y, Asahina K, Asahara T & Yoshizato K 2005 Efficient *in vivo* xenogeneic retroviral vector-mediated gene transduction into human hepatocytes. *Human Gene Therapy* **16** 1168–1174.

Fausto N 2000 Liver regeneration. *Journal of Hepatology* **32** 19–31.

Gronowski AM & Rotwein P 1994 Rapid changes in nuclear protein tyrosine phosphorylation after growth hormone treatment *in vivo*. *Journal of Biological Chemistry* **269** 7874–7878.

Gronowski AM, Zhonq Z, Wen Z, Thomas MJ, Darnell JE Jr & Rotwein P 1995 *In vivo* growth hormone treatment rapidly stimulates the tyrosine phosphorylation and activation of Stat3. *Molecular Endocrinology* **9** 171–177.

Herrington J, Smit LS, Schwartz J & Carter-Su C 2000 The role of STAT proteins in growth hormone signaling. *Oncogene* **19** 2585–2597.

Kelijman M 1991 Age-related alterations of the growth hormone/insulin-like-growth-factor I axis. *Journal of the American Geriatrics Society* **39** 295–307.

Krupczak-Hollis K, Wang X, Dennewitz MB & Costa RH 2003 Growth hormone stimulates proliferation of old-aged regenerating liver through Forkhead Box m1b. *Hepatology* **38** 1552–1562.

Livak KJ & Schmittgen TD 2001 Analysis of relative gene expression data using real-time quantitative PCR and the $2^{-\Delta\Delta C_T}$ method. *Methods* **25** 402–408.

Major ML, Lepe R & Costa RH 2004 Forkhead Box M1B (FoxM1B) transcriptional activity requires binding of Cdk/cyclin complexes for phosphorylation-dependent recruitment of p300/CBP co-activators. *Molecular and Cellular Biology* **24** 2649–2661.

Mars WM, Liu ML, Kitson RP, Goldfarb RH, Gabauer MK & Michalopoulos GK 1995 Immediate early detection of urokinase receptor after partial hepatectomy and its implications for initiation of liver regeneration. *Hepatology* **21** 1695–1701.

Massague J 2004 G1 cell-cycle control and cancer. *Nature* **432** 298–306.

Meuleman P, Vanlandschoot P & Leroux-Roels G 2003 A simple and rapid method to determine the zygosity of uPA-transgenic SCID mice. *Biochemical and Biophysical Research Communications* **308** 375–378.

Michalopoulos GK & DeFrances MC 1997 Liver regeneration. *Science* **276** 60–66.

Pennisi PA, Kopchick JJ, Thorgeirsson S, LeRoith D & Yakar S 2004 Role of growth hormone (GH) in liver regeneration. *Endocrinology* **145** 4748–4755.

Sebastian B, Kakizuka A & Hunter T 1993 Cdc25M2 activation of cyclin-dependent kinases by dephosphorylation of threonine-14 and tyrosine-15. *PNAS* **90** 3521–3524.

Sjogren K, Liu JL, Blad K, Skrtic S, Vidal O, Wallenius V, LeRoith D, Tornell J, Isaksson OG, Jansson JO *et al.* 1999 Liver-derived insulin-like growth factor I (IGF-I) is the principal source of IGF-I in blood but is not required for postnatal body growth in mice. *PNAS* **96** 7088–7092.

Souza SC, Frick GP, Wang X, Kopchick JJ, Lobo RB & Goodman HM 1995 A single arginine residue determines species specificity of the human growth hormone receptor. *PNAS* **92** 959–963.

Stocker E & Heine WD 1971 Regeneration of liver parenchyma under normal and pathological conditions. *Beiträge zur Pathologie* **144** 400–408.

Tateno C, Yoshizane Y, Saito N, Kataoka M, Utoh R, Yamasaki C, Tachibana A, Soeno Y, Asahina K, Hino H *et al.* 2004 Near completely humanized liver in mice shows human-type metabolic responses to drugs. *American Journal of Pathology* **165** 901–912.

Taub R 1996 Liver regeneration 4: transcriptional control of liver regeneration. *FASEB Journal* **10** 413–427.

Tsuge M, Hiraga N, Takaishi H, Noguchi C, Oga H, Imamura M, Takahashi S, Iwao E, Fujimoto Y, Ochi H *et al.* 2005 Infection of human hepatocyte chimeric mouse with genetically engineered hepatitis B virus. *Hepatology* **42** 1046–1054.

Wang X, Quail E, Hung NJ, Tan Y, Ye H & Costa RH 2001 Increased levels of Forkhead box M1B transcription factor in transgenic mouse hepatocytes prevent age-related proliferation defects in regenerating liver. *PNAS* **98** 11468–11473.

Wang X, Kiyokawa H, Dennewitz MB & Costa RH 2002*a* The Forkhead Box M1B transcription factor is essential for hepatocyte DNA replication and mitosis during mouse liver regeneration. *PNAS* **99** 16881–16886.

Wang X, Krupczak-Hollis K, Tan Y, Dennewitz MB, Adami GR & Costa RH 2002*b* Increased hepatic Forkhead Box M1B (FoxM1B) levels in old-aged mice stimulated liver regeneration through diminished $p27^{kip1}$ protein levels and increased Cdc25B expression. *Journal of Biological Chemistry* **277** 44310–44316.

Wang IC, Chen YJ, Hughes D, Petrovic V, Major ML, Park HJ, Tan Y, Ackerson T & Costa RH 2005 Forkhead Box M1 regulates the transcriptional network of genes essential for mitotic progression and genes encoding the SCF (Skp2-Cks1) ubiquitin ligase. *Molecular and Cellular Biology* **25** 10875–10894.

Xu X, Bennett SA, Ingram RL & Sonntag WE 1995 Decreases in growth hormone receptor signal transduction contribute to the decline in insulin-like growth factor I gene expression with age. *Endocrinology* **136** 4551–4557.

Yakar S, Liu JL, Stannard B, Butler A, Accili D, Sauer B & LeRoith D 1999 Normal growth and development in the absence of hepatic insulin-like growth factor I. *PNAS* **96** 7324–7329.

Received in final form 3 June 2007
Accepted 7 June 2007
Made available online as an Accepted Preprint
12 June 2007

Cytometry

Single Lymphocyte Analysis with a Microwell Array Chip

Yoshiharu Tokimitsu,[1,2] Hiroyuki Kishi,[1*] Sachiko Kondo,[1] Ritsu Honda,[1] Kazuto Tajiri,[1,2] Kazumi Motoki,[1] Tatsuhiko Ozawa,[1] Shinichi Kadowaki,[1] Tsutomu Obata,[3] Satoshi Fujiki,[3] Chise Tateno,[4] Hideki Takaishi,[5] Kazuaki Chayama,[5] Katsutoshi Yoshizato,[6] Eiichi Tamiya,[7] Toshiro Sugiyama,[2] Atsushi Muraguchi[1]

[1]Department of Immunology, Graduate School of Medicine and Pharmaceutical Sciences, University of Toyama, Toyama, Japan

[2]The Third Department of Internal Medicine, Graduate School of Medicine and Pharmaceutical Sciences, University of Toyama, Toyama, Japan

[3]The Central Institute, Toyama Industrial Technology Center, Takaoka, Toyama, Japan

[4]The Yoshizato Project, CLUSTER, Hiroshima Prefectural Institute of Industrial Science and Technology, Higashi-Hiroshima, Japan

[5]Department of Medicine and Molecular Science, Division of Frontier Medical Science, Graduate School of Biomedical Sciences, Hiroshima University, Hiroshima, Japan

[6]Developmental Biology Laboratory, Department of Biological Science, Graduate School of Science, Hiroshima University, Higashi-Hiroshima, Japan

[7]Department of Applied Physics, Osaka University, Suita, Osaka, Japan

*Correspondence to: Hiroyuki Kishi, Department of Immunology, Graduate School of Medicine and Pharmaceutical Sciences, University of Toyama, 2630 Sugitani, Toyama 930-0194, Japan

Email: immkishi@med.u-toyama.ac.jp

Published online 30 October 2007 in Wiley InterScience (www.interscience.wiley.com)

DOI: 10.1002/cyto.a.20478

• Abstract

Following genomics and proteomics, cytomics, a novel method of looking at life, has emerged for analyzing large populations of cells on a single-cell basis with multiple parameters in a quantitative manner. We have developed a highly integrated live-cell microarray system for analyzing the cellular responses of individual cells using a microwell array chip that has 234,000 microwells each of which is just large enough to fit a single cell. Compared with flow cytometry and microscope-based methods, our system can analyze the history of the cellular responses of a large number of cells. We have successfully applied the system to analyze human antigen-specific B-cells and produced human monoclonal antibodies (MoAb) against hepatitis B virus surface antigen. We have also constructed a mouse system to assess hepatitis B virus-neutralization activity and have demonstrated the neutralization activity of our antibodies. Our technology should expand the horizons of cell analysis as well as enable generation of human MoAb for antibody-based therapeutics and diagnosis for infectious diseases such as hepatitis viruses.

• Key terms

lymphocyte; microwell array chip; monoclonal antibody; hepatitis B virus; intracellular calcium

CYTOMICS is a novel perspective from which to look at life and to study the "cytome," analyzing large populations of cells on a single-cell basis with multiple parameters in a quantitative and observer-independent manner (1). To meet the discipline of cytomics, sensitive fluorescence detection devices and sophisticated image analysis procedures have been developed, including tools based on flow cytometry or those based on microscopy (2). Flow cytometers have enabled us to analyze fluorescent signals of large numbers of cells flowing through sheath fluid, but they cannot track the history of the fluorescent signals from each cell of interest. In contrast, tools based on microscopes have enabled us to analyze signals of individual cells at various time points. However, we cannot analyze a large number of cells with a microscope, especially when cells are nonadherent.

B-cells, a major cell population in immune systems, produce antibodies that specifically recognize antigens, such as infectious microbes, neutralize their infectivity, and eliminate them by various immune effector mechanisms. B-cells express mono-specific antibodies on the cell surface as antigen receptors that recognize extra-cellular antigens. It has been estimated that an individual human contains on the order of 10^7 clones of B-cells with distinct specificities (3). It has also been reported that the frequencies of antigen-specific B-cells are quite diverse, which may be due to the form of immunogen. For example, more than 10% of B-cells produce

ISAC International Society for Analytical Cytology